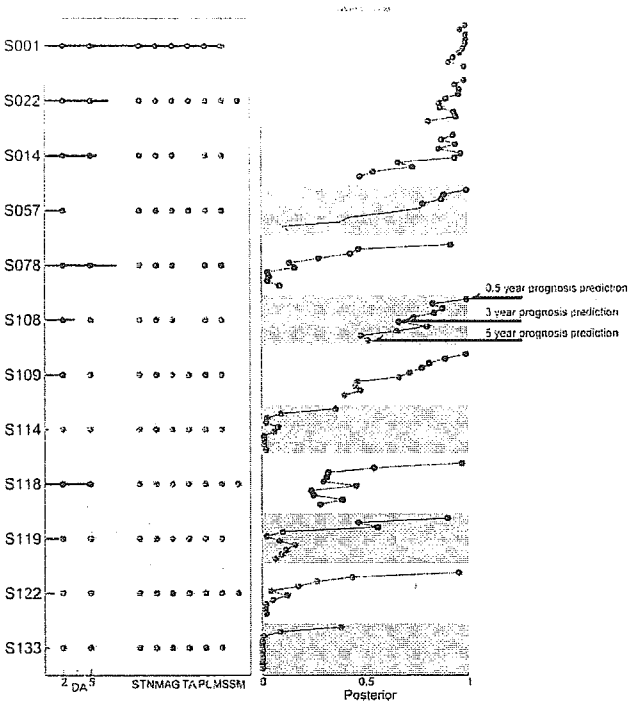

Figure 6. Individual survival chance analysis based on posterior probabilities

LTO estimation of survival probabilities at 0.5, 1.0, 1.5, ..., 5.0 years after diagnosis for 12 typical patients. Left panel: Information of patients (see caption of Figure 2). Right panel: Estimated posterior probabilities at 0.5, 1.0, 1.5, ..., 5.0 years after diagnosis, which predict the time course of patient's survival chance. A blue or a red mark denotes that the patient is alive or dead at that time after diagnosis, respectively. For example, the patient "S108," who died at 40 months, is predicted as 100% alive at 0.5 year and 52% alive at 5 year, solely from the microarray analysis at the diagnosis

The high outcome predictability of our system is attributable to multiple reasons. The quality of tumor samples is high because (1) an appropriate system was established for our neuroblastoma tissue bank, and (2) handling of tumor tissues is rather uniform at each hospital, in which informed consent was obtained. An array, produced by a new apparatus equipped with a piezo microceramic pump, generates highly reproducible signals. The noncontact spotting method makes the spot shape almost a perfect circle. Consequently, the spot excels in signal uniformity. We did not conduct microdissection of the 136 tumor samples, because the stromal components of the tumor, e.g., Schwannian cells, are already known to be very important to characterize its biology (Ambros and Ambros, 1995; Ambros and Ambros, 2000). Therefore, a good combination or selection of these procedures may have provided high outcome predictability. In addition, the high predictability was reliably confirmed by the complete crossvalidation analysis and the independent test. The probabilistic output based on the LTO analysis can provide a new type of information that will improve the therapeutic decision at the bedside. In addition, the probabilistic output is highly robust against noises that may be involved in test samples (described above); this can be the major reason for the high prediction accuracy when the classifier constructed by the 5340 genes system was applied to the data taken by the mini-chip system.

The impact of the selected genes is strong. The genes with the highest score in F group genes (F > UF) were *tubulin* α members (*TUBA3* and *K-ALPHA-1*, which corresponds to *TUBA1*), which have never been reported to be prognostic factors in neuroblastoma. Their prognostic significance has also been confirmed by RT-PCR in primary tumors (data not shown). The high expression of *TUBA1* in neuronal cells is associated with axonal outgrowth during development as well as with axonal degeneration after axotomy in adult animals (Knoops and Octave, 1997). The expression of *TUBA3* has been reported to be restricted to adherent, morphologically differentiated neuronal and glial cells (Hall and Cowan, 1985). We have also found that high expression of *tubulin tyrosine ligase* and enhanced tubulin tyrosination/detyrosination cycle are associated with neuronal differentiation in neuroblastomas with favorable prognosis (Kato et al., 2004). Thus, high mRNA expression of *TUBA* genes in favorable neuroblastoma may reflect differentiated status of tumors. ARHGEF7, Rho guanine nucleotide exchange factor 7, activates Rho proteins by exchanging bound GDP for GTP and can induce membrane ruffling. In our previous paper, we found that many family members of such G protein-related genes are highly expressed in favorable neuroblastomas compared to unfavorable ones (Ohira et al., 2003a). This may also imply a neuronal maturity nature of favorable tumors. Peripherin, a type III intermediate filament protein, was initially found as a cytoskeletal protein in the peripheral nervous system and in cultured cells of neuronal origin. This protein is known to be a marker of terminal neuronal differentiation; however, its functional role in neuroblastoma has been elusive. The previous evidence indicates that peripherin is transcriptionally upregulated by treatment with NGF, an important neurotrophin in neuroblastoma, and that the protein product is directly phosphorylated by NGF receptor, TrkA (Aletta et al., 1989). Thus, peripherin may play an important role as one of the signal transduction components involved in elaboration and maintenance of neuronal differentiation. In the UF gene group, many ribosomal protein-related genes are selected. *GNB2L1*, a receptor for activated C-kinase *RACK1*, is implicated in linking between *PKC* signaling and ribosome activation (Ceci et al., 2003). The *DDX1* gene, which is frequently coamplified with the *MYCN* gene in advanced neuroblastomas (Godbout and Squire, 1993; Noguchi et al., 1996), is also a member of this group. Its protein product is a putative RNA helicase and is implicated in a number of cellular processes involving alteration of RNA secondary structure such as translation initiation, nuclear and mitochondrial splicing, and ribosome and spliceosome assembly. *DDX1* is ranked at a higher score than the *MYCN* gene, which is concordant with the previous reports describing that *MYCN* mRNA expression is a weaker prognostic marker than its genomic amplification (Slavc et al., 1990). Another important prognostic factor, *TrkA*, is not included in the top 70 genes but in the 90 (in the top 20 genes when the 5 year label was used) (data not shown), probably due to its relatively low levels of mRNA expression as compared with those of other genes. The prognos-

tic effect of *TrkA* expression may be compensated by other genes which are affected or regulated by *TrkA* intracellular signaling. Similarly, *MYCN*-regulated genes such as ribosomal genes, translation initiation and elongation factors, and laminin receptor may compensate the effect of *MYCN* gene expression in aggressive tumors. It is intriguing that high mRNA expression of *p53* gene is also strongly related to unfavorable outcome. Although *p53* mutation is rare in primary neuroblastomas, and its gene product frequently accumulated in cytoplasm, an unknown mechanism that upregulates *p53* expression in aggressive tumors may exist.

Our results showed that the decision by majority by the genes selected based on microarray data alone can be a prognostic indicator comparative to the existing prognostic markers, and that the addition of the microarray data to the prognosis markers improved the outcome prediction (Table 1). The outcomes of patients belonging to the intermediate subset, whose prognosis prediction had been very difficult by existing prognosis markers, were effectively separated into favorable group and unfavorable group ($p < 10^{-4}$). The posterior value will help the decision of therapeutic modalities, and outcome prediction based on the posterior value is extremely robust against a possible noise. In addition, our practical, low-cost microarray carrying only 200 genes should make its clinical use possible. Our further validation by hybridizing RNA obtained from 50 fresh neuroblastomas on the 200 cDNAs microarray in a completely independent laboratory indicated that our prediction system is consistent and feasible. Therefore, the application of a highly qualified cDNA microarray at the bedside may bring tailored medicine that allows better treatment of neuroblastoma patients.

Experimental procedures

Patients and tumor specimens

Fresh, frozen tumor tissues were sent to the Division of Biochemistry, Chiba Cancer Center Research Institute, from a number of hospitals in Japan (1996–2002). Informed consent was obtained at each institution or hospital. We randomly selected tumor samples from this neuroblastoma tissue bank and then successfully conducted hybridization in 136 neuroblastomas consisting of 41 stage 1 tumors, 22 stage 2 tumors, 33 stage 3 tumors, 28 stage 4 tumors, and 12 stage 4s tumors. Among the 136 fresh neuroblastomas, seventeen tumors were obtained at the delayed primary surgery after giving chemotherapy, but the other 119 tumors were resected by biopsy or surgery without giving any therapy. After surgery, patients were treated according to the previously described common protocols (Kaneko et al., 1998). Biological information on each tumor, including *MYCN* gene copy number, *TrkA* gene expression, and DNA ploidy, was analyzed in our laboratory, as described previously (Hishiki et al., 1998). All the tumors were classified according to the International Neuroblastoma Staging System (INSS) (Brodeur et al., 1993). The stage 4s neuroblastoma shows a special pattern of clinical behaviors, and the tumor itself, as well as its widespread metastases to the skin, liver, or bone marrow, usually regresses spontaneously. For a better understanding of statistical results, we introduced Brodeur's classification of neuroblastoma subsets: type I (stages 1, 2, or 4s; a single copy of *MYCN*; blue marks in Figure 2), type II (stage 3 or 4; a single copy of *MYCN*; green marks in Figure 2), and type III (all stages; amplification of *MYCN*; red marks in Figure 2) (Brodeur and Nakagawara, 1992). Among 136 tumors that we analyzed, 66 were found by mass screening of urinary catecholamine metabolites at the age of 6 months, which has been performed nationwide in Japan from 1984 to 2004 (Sawada et al., 1984). The follow-up duration ranged between 3 and 241 months (median, 56 months; mean, 57.3 months) after diagnosis. All diagnoses of neuroblastoma were confirmed by the histological assessment of a surgically resected tumor specimen at each hospital. Shimada's classification (Shimada et al., 1984) was performed in 62 out of 136 cases. The macroscopic necroses in the tumor were excluded from the tissue sampling for molecular analysis. We used for the microarray analysis only the tumor samples whose adjacent tissues contained more than 70% tumor cells in the thin sections stained with hematoxylin-eosin. For independent test, 50 (19 were found by mass screening and 31 were clinically found) tumors (15 of stage 1, 6 of stage 2, 9 of stage 3, 14 of stage 4, and 6 of stage 4s) were used.

Total RNA was extracted from each frozen tissue according to the AGPC method (Chomczynski and Sacchi, 1987). RNA integrity, quality, and quantity were then assessed by electrophoresis on the Agilent RNA 6000 nanochip using Agilent 2100 BioAnalyzer (Agilent Technologies, Inc.).

cDNA microarray experiments

We previously obtained approximately 5,000 genes after selecting from 10,000 clones randomly picked up from the mixture of oligo-capping cDNA libraries, which were generated from three primary neuroblastomas with a favorable outcome (stage 1; high *TrkA* expression and a single copy of *MYCN*), three tumors with a poor prognosis (stage 3 or 4; low expression of *TrkA* and amplification of *MYCN*), and a stage 4s tumor (Ohira et al., 2003a; Ohira et al., 2003b). Using these isolated genes together with 80 known cDNAs that were thought to be neuroblastoma-related genes, we first constructed a neuroblastoma proper cDNA microarray (named CCC-NB5000-Chip) carrying 5340 cDNA spots (the 5340 genes system). Insert DNAs (average size, approximately 2.5kb) were amplified by polymerase chain reaction (PCR) from these cDNA clones, purified by ethanol precipitation, and spotted onto a glass slide at a high density with an ink-jet printing tool (NGK Insulators, Ltd.).

Ten micrograms each of total RNA were labeled with the CyScribe RNA labeling kit in accordance with the manufacturer's manual (Amersham Pharmacia Biotech), followed by probe purification with the Qiagen MinElute PCR purification kit (Qiagen). We used a mixture of equal amounts of RNA from each of four neuroblastoma cell lines (NB69, NBL-S, SK-N-AS, and SH-SY5Y) as a reference. RNAs extracted from primary neuroblastoma tissues and RNAs of the reference mixture were labeled with Cy3 and Cy5 dye, respectively, and were used as probes together with yeast tRNA and polyA for suppression. Subsequent hybridization and washing were conducted as described previously (Takahashi et al., 2002; Yoshikawa et al., 2000). Hybridized microarrays were scanned using the Agilent G2505A confocal laser scanner (Agilent Technologies, Inc.), and fluorescent intensities were quantified using the GenePix Pro microarray analysis software (Axon Instruments, Inc.). The procedure of this study was approved by the Institutional Review Board of the Chiba Cancer Center.

After selecting genes strongly related to the prognosis of patients with neuroblastoma (at 2 years and at 5 years after diagnosis), we constructed a 200 cDNAs microarray on glass slides by the same procedure described above (the mini-chip system). For the independent test using 50 samples, tumor RNA preparation, probe labeling, and hybridization were conducted in a completely different laboratory from the original 136 hybridization. In this independent test, 5 μg each of total RNA were used for labeling.

Data preprocessing

To remove chip-wise biases of a microarray system, we used the LOWESS normalization (Cleveland, 1979). When the Cy3 or Cy5 strength for a clone was smaller than 3, strength was regarded as abnormally small, and the log expression ratio of the corresponding clone was treated as a missing value. The rate of such missing entries was less than 1%. After normalizing the 5340 (genes) by 136 (samples) log expression matrix and removing missing values, each missing entry was imputed to an estimated value by Bayesian principal component analysis, which was developed previously (Oba et al., 2003).

Supervised machine learning and LTO crossvalidation

The 96 samples, whose prognosis at 5 years after diagnosis had been successfully checked, were used to train a supervised classifier that predicts the 5 year prognosis of a new patient. When we considered the short-term prediction, 126 samples whose 2 year prognosis is known were used. Selection of the genes that are related to the classification is an important preprocess for reliable prediction. We omitted the genes whose standard

deviation of the log ratios for the genes obtained over 136 experiments was smaller than 0.36, so that 1000 genes remained, because the background noise level was about 0.2–0.3. After the gene screening, the genes were scored by the pairwise *F* score, which is a modification of a pairwise correlation method (Bo and Jonassen, 2002), to conduct gene ranking in an attempt not only to obtain higher discrimination accuracy by using a smaller number of genes but also to reserve the applicability to various outcome prediction by the set of selected genes (see the Supplemental Data).

We used a well-established technique in the supervised classification (prognosis prediction), that is, weighted voting with linear discriminators, where each weight value was calculated as the signal-to-noise ratio (Golub et al., 1999). In the weighted voting, only n genes with the largest pairwise *F* score were used. The number of top genes, n, strongly affects the prediction accuracy (Figure S3) as found in various microarray studies and hence should be determined such to maximize the leave one out (LOO) crossvalidation accuracy. However, a naive determination process of n may introduce information leakage, and the accuracy optimized by the LOO crossvalidation involves overestimation. To avoid such an overestimation, we consulted a LTO analysis. The LTO analysis was constituted of inner and outer loops of LOO (Figure S2A); the gene number n was optimized by the LOO crossvalidation repeating the inner loops, and the optimized classifier was evaluated by an independent test for a single sample left out at a single step in the outer loop. During repetition of such steps, the test results of the outer loop were never fed back to the classifier's optimization process in the inner loops, and hence the tests in the outer loop did not include any overestimation, and the estimated accuracy involved the smallest bias as possible.

The posterior value for a single sample was calculated based on the distribution of the weighted vote (decision by majority by the genes that join the vote) *f* within the LTO analysis. We regard a real-valued weighted vote as carrying two kinds of information: its sign predicts the label (favorable or unfavorable) of the corresponding sample, and its absolute value shows the prediction strength. The posterior probability p for this sample being favorable (alive at 5 years) was evaluated as the logit transformation $p = \exp(\beta_0 + \beta_1 f)/[1 + \exp(\beta_0 + \beta_1 f)]$, where parameters β_0 and β_1 were estimated by the maximum likelihood method, in each step in the outer loop of LTO using the remaining 95 samples and the corresponding labels (5 year prognosis). Then, the posterior probability of the sample left out in the outer loop was predicted by the weighted vote *f* by the classifier constructed in the inner LOO loops and the parameters β_0 and β_1 obtained above. There is therefore no information leakage in this calculation process of the posterior of the sample left out.

Independent test

Using the 50 independent samples, we performed two kinds of tests. The first one is an independent test to validate the classifier obtained by our method and the applicability of our classifier to the mini-chip system, which has been developed as a clinical tool at the bedside (Figure S2B). According to the LTO analysis, the supervised classifier was finally constructed by using all of the 96 training samples measured by the 5340 genes system. This classifier was evaluated by being directly applied to the 50 samples measured by the mini-chip system without any information from measurements by the mini-chip system and the 50 test samples. In this test, tumor RNA preparation, probe labeling, and hybridization were conducted in a completely different laboratory from that for the 5340 genes system. The second one is to validate the LTO analysis to construct a supervised classifier by applying the procedure to the data taken by the mini-chip system.

Survival analysis

The Kaplan-Meier survival analysis was also programmed and used to compare patient survival. To assess the association of selected gene expression with patient clinical outcome, the statistical p and q values were calculated based on the log rank test.

Immunohistochemistry

Immunostaining with the antibody against peripherin protein (Santa Cruz Biotechnology; 1:400) was performed on six human neuroblastoma tumors selected from the surgical pathology file at the Department of Pathology, Aichi Medical University. They were all neuroblastoma (Schwannian stroma–poor) and included three favorable histology tumors (poorly differentiated subtype without *MYCN* amplification [one case]; differentiated subtype without *MYCN* amplification [two cases]) and three unfavorable histology tumors (undifferentiated subtype without *MYCN* amplification [one case]; poorly differentiated subtype with *MYCN* amplification [one case]; poorly differentiated subtype without *MYCN* amplification). All tumor tissues were obtained prior to chemotherapy and irradiation therapy. Four micron thick sections from the formalin-fixed, paraffin-embedded samples of these tumors were treated according to the protocol described previously (Kato et al., 2004). As for the negative controls, normal goat immunoglobulins (1:500 dilution; Vector Laboratories) were applied as the primary antibody.

Supplemental data

The Supplemental Data include Supplemental Experimental Procedures and ten supplemental figures and can be found with this article online at http://www.cancercell.org/cgi/content/full/7/4/337/DC1/.

Acknowledgments

We are grateful to the hospitals and institutions that provided us with surgical specimens (see the Supplemental Data). We also thank Shigeru Sakiyama and John K. Cowell for reading the manuscript; Naohiko Seki, Tsutomu Yoshikawa, and Masaki Kato for their valuable suggestions; and Natsue Kitabayashi, Tomonori Saito, Naoko Sugimitsu, Yuki Nakamura, Naoko Shibano, Emiko Kojima, Hisae Murakami, and Kazumi Yagyu for their technical support. This work was supported in part by a fund from Hisamitsu Pharmaceutical Co., Inc.; by Grants-in-Aid for Scientific Research on Priority Areas (C) "Medical Genome Science" and "Genome Information Science" and for Scientific Research (B) from the Ministry of Education, Culture, Sports, Science and Technology of Japan; and by Grant-in Aid for Cancer Research from the Ministry of Health, Labor and Welfare of Japan.

Received: November 17, 2003
Revised: January 8, 2005
Accepted: March 11, 2005
Published: April 18, 2005

References

Aletta, J.M., Shelanski, M.L., and Greene, L.A. (1989). Phosphorylation of the peripherin 58-kDa neuronal intermediate filament protein. J. Biochem. (Tokyo) *264*, 4619–4627.

Ambros, I.M., and Ambros, P.F. (1995). Schwann cells in neuroblastoma. Eur. J. Cancer *4*, 429–434.

Ambros, I.M., and Ambros, P.F. (2000). The role of Schwann cells in neuroblastoma. In Neuroblastoma, G.M. Brodeur, T. Sawada, Y. Tsuchida, and P.A. Voute, eds. (Amsterdam: Elsevier), pp. 229–243.

Beer, D.G., Kardia, S.L., Huang, C.C., Giordano, T.J., Levin, A.M., Misek, D.E., Lin, L., Chen, G., Gharib, T.G., Thomas, D.G., et al. (2002). Gene-expression profiles predict survival of patients with lung adenocarcinoma. Nat. Med. *8*, 816–824.

Berwanger, B., Hartmann, O., Bergmann, E., Bernard, S., Nielsen, D., Krause, M., Kartal, A., Flynn, D., Wiedemeyer, R., Schwab, M., et al. (2002). Loss of a FYN-regulated differentiation and growth arrest pathway in advanced stage neuroblastoma. Cancer Cell *2*, 377–386.

Bo, T., and Jonassen, I. (2002). New feature subset selection procedures for classification of expression profiles. Genome Biol. *3*, RESEARCH0017.

Bolande, R.P. (1974). The neurocristopathies: a unifying concept of disease arising in neural crest maldevelopment. Hum. Pathol. *5*, 409–429.

Brodeur, G.M., and Nakagawara, A. (1992). Molecular basis for clinical heterogeneity in neuroblastoma. Am. J. Pediatr. Hematol. Oncol. *14*, 111–116.

Brodeur, G.M., Seeger, R.C., Schwab, M., Varmus, H.E., and Bishop, J.M.

(1984). Amplification of N-myc in untreated human neuroblastomas correlates with advanced disease stage. Science *224*, 1121–1124.

Brodeur, G.M., Fong, C.T., Morita, M., Griffith, R., Hayes, F.A., and Seeger, R.C. (1988). Molecular analysis and clinical significance of N-myc amplification and chromosome 1p monosomy in human neuroblastomas. Prog. Clin. Biol. Res. *271*, 3–15.

Brodeur, G.M., Pritchard, J., Berthold, F., Carlsen, N.L., Castel, V., Castelberry, R.P., De Bernardi, B., Evans, A.E., Favrot, M., Hedborg, F., et al. (1993). Revisions of the international criteria for neuroblastoma diagnosis, staging, and response to treatment. J. Clin. Oncol. *11*, 1466–1477.

Ceci, M., Gaviraghi, C., Gorrini, C., Sala, L.A., Offenhauser, N., Marchisio, P.C., and Biffo, S. (2003). Release of eIF6 (p27BBP) from the 60S subunit allows 80S ribosome assembly. Nature *426*, 579–584.

Chomczynski, P., and Sacchi, N. (1987). Single-step method of RNA isolation by acid guanidinium thiocyanate-phenol-chloroform extraction. Anal. Biochem. *162*, 156–159.

Cleveland, W.S. (1979). Robust locally weighted regression and smoothing scatterplots. J. Am. Stat. Assoc. *74*, 829–836.

Evans, A.E., D'Angio, G.J., and Randolph, J. (1971). A proposed staging for children with neuroblastoma. Children's cancer study group A. Cancer *27*, 374–378.

Favrot, M.C., Combaret, V., and Lasset, C. (1993). CD44—a new prognostic marker for neuroblastoma. N. Engl. J. Med. *329*, 1965.

Godbout, R., and Squire, J. (1993). Amplification of a DEAD box protein gene in retinoblastoma cell lines. Proc. Natl. Acad. Sci. USA *90*, 7578–7582.

Golub, T.R., Slonim, D.K., Tamayo, P., Huard, C., Gaasenbeek, M., Mesirov, J.P., Coller, H., Loh, M.L., Downing, J.R., Caligiuri, M.A., et al. (1999). Molecular classification of cancer: class discovery and class prediction by gene expression monitoring. Science *286*, 531–537.

Hall, J.L., and Cowan, N.J. (1985). Structural features and restricted expression of a human α-tubulin gene. Nucleic Acids Res. *13*, 207–223.

Hishiki, T., Nimura, Y., Isogai, E., Kondo, K., Ichimiya, S., Nakamura, Y., Ozaki, T., Sakiyama, S., Hirose, M., Seki, N., et al. (1998). Glial cell line-derived neurotrophic factor/neurturin-induced differentiation and its enhancement by retinoic acid in primary human neuroblastomas expressing c-Ret, GFR α-1, and GFR α-2. Cancer Res. *58*, 2158–2165.

Hiyama, E., Hiyama, K., Yokoyama, T., Matsuura, Y., Piatyszek, M.A., and Shay, J.W. (1995). Correlating telomerase activity levels with human neuroblastoma outcomes. Nat. Med. *1*, 249–255.

Iizuka, N., Oka, M., Yamada-Okabe, H., Nishida, M., Maeda, Y., Mori, N., Takao, T., Tamesa, T., Tangoku, A., Tabuchi, H., et al. (2003). Oligonucleotide microarray for prediction of early intrahepatic recurrence of hepatocellular carcinoma after curative resection. Lancet *361*, 923–929.

Kaneko, M., Nishihira, H., Mugishima, H., Ohnuma, N., Nakada, K., Kawa, K., Fukuzawa, M., Suita, S., Sera, Y., and Tsuchida, Y. (1998). Stratification of treatment of stage 4 neuroblastoma patients based on N-myc amplification status. Study Group of Japan for Treatment of Advanced Neuroblastoma, Tokyo, Japan. Med. Pediatr. Oncol. *31*, 1–7.

Kato, C., Miyazaki, K., Nakagawa, A., Ohira, M., Nakamura, Y., Ozaki, T., Imai, T., and Nakagawara, A. (2004). High expression of human tubulin tyrosine ligase and enhanced tubulin tyrosination/detyrosination cycle are associated with neuronal differentiation in neuroblastomas with favorable prognosis. Int. J. Cancer *112*, 365–375.

Knoops, B., and Octave, J.N. (1997). α1-tubulin mRNA level is increased during neurite outgrowth of NG 108-15 cells but not during neurite outgrowth inhibition by CNS myelin. Neuroreport *8*, 795–798.

Look, A.T., Hayes, F.A., Nitschke, R., McWilliams, N.B., and Green, A.A. (1984). Cellular DNA content as a predictor of response to chemotherapy in infants with unresectable neuroblastoma. N. Engl. J. Med. *311*, 231–235.

Look, A.T., Hayes, F.A., Shuster, J.J., Douglass, E.C., Castleberry, R.P., Bowman, L.C., Smith, E.I., and Brodeur, G.M. (1991). Clinical relevance of tumor cell ploidy and N-myc gene amplification in childhood neuroblastoma: a Pediatric Oncology Group study. J. Clin. Oncol. *9*, 581–591.

Nagata, T., Takahashi, Y., Asai, S., Ishii, Y., Mugishima, H., Suzuki, T., Chin, M., Harada, K., Koshinaga, S., and Ishikawa, K. (2000). The high level of hCDC10 gene expression in neuroblastoma may be associated with favorable characteristics of the tumor. J. Surg. Res. *92*, 267–275.

Nakagawara, A., Arima, M., Azar, C.G., Scavarda, N.J., and Brodeur, G.M. (1992). Inverse relationship between trk expression and N-myc amplification in human neuroblastomas. Cancer Res. *52*, 1364–1368.

Nakagawara, A., Arima-Nakagawara, M., Scavarda, N.J., Azar, C.G., Cantor, A.B., and Brodeur, G.M. (1993). Association between high levels of expression of the TRK gene and favorable outcome in human neuroblastoma. N. Engl. J. Med. *328*, 847–854.

Nakagawara, A., Milbrandt, J., Muramatsu, T., Deuel, T.F., Zhao, H., Cnaan, A., and Brodeur, G.M. (1995). Differential expression of pleiotrophin and midkine in advanced neuroblastomas. Cancer Res. *55*, 1792–1797.

Noguchi, T., Akiyama, K., Yokoyama, M., Kanda, N., Matsunaga, T., and Nishi, Y. (1996). Amplification of a DEAD box gene (DDX1) with the MYCN gene in neuroblastomas as a result of cosegregation of sequences flanking the MYCN locus. Genes Chromosomes Cancer *15*, 129–133.

Ntzani, E.E., and Ioannidis, J.P. (2003). Predictive ability of DNA microarrays for cancer outcomes and correlates: an empirical assessment. Lancet *362*, 1439–1444.

Oba, S., Takemasa, N., Monden, M., Matsubara, K., and Ishii, S. (2003). A Bayesian missing value estimation method. Bioinformatics *19*, 2088–2096.

Ohira, M., Morohashi, A., Inuzuka, H., Shishikura, T., Kawamoto, T., Kageyama, H., Nakamura, Y., Isogai, E., Takayasu, H., Sakiyama, S., et al. (2003a). Expression profiling and characterization of 4200 genes cloned from primary neuroblastomas: identification of 305 genes differentially expressed between favorable and unfavorable subsets. Oncogene *22*, 5525–5536.

Ohira, M., Morohashi, A., Nakamura, Y., Isogai, E., Furuya, K., Hamano, S., Machida, T., Aoyama, M., Fukumura, M., Miyazaki, K., et al. (2003b). Neuroblastoma oligo-capping cDNA project: toward the understanding of the genesis and biology of neuroblastoma. Cancer Lett. *197*, 63–68.

Sawada, T., Hirayama, M., Nakata, T., Takeda, T., Takasugi, N., Mori, T., Maeda, K., Koide, R., Hanawa, Y., Tsunoda, A., et al. (1984). Mass screening for neuroblastoma in infants in Japan. Interim report of a mass screening study group. Lancet *2*, 271–273.

Schwab, M., Alitalo, K., Klempnauer, K.H., Varmus, H.E., Bishop, J.M., Gilbert, F., Brodeur, G., Goldstein, M., and Trent, J. (1983). Amplified DNA with limited homology to myc cellular oncogene is shared by human neuroblastoma cell lines and a neuroblastoma tumour. Nature *305*, 245–248.

Shimada, H., Chatten, J., Newton, W.A., Sachs, N., Hamoudi, A.B., Chiba, T., Marsden, H.B., and Misugi, K. (1984). Histopathologic prognostic factors in neuroblastic tumors; definition of subtypes of ganglioneuroblastoma and an age-linked classification of neuroblastomas. J. Natl. Cancer Inst. *73*, 405–416.

Shimono, R., Matsubara, S., Takamatsu, H., Fukushige, T., and Ozawa, M. (2000). The expression of cadherins in human neuroblastoma cell lines and clinical tumors. Anticancer Res. *20*, 917–923.

Slavc, I., Ellenbogen, R., Jung, W.H., Vawter, G.F., Kretschmar, C., Grier, H., and Korf, B.R. (1990). myc gene amplification and expression in primary human neuroblastoma. Cancer Res. *50*, 1459–1463.

Storey, J.D., and Tibshirani, R. (2003). Statistical significance for genome-wide studies. Proc. Natl. Acad. Sci. USA *100*, 9440–9445.

Takahashi, M., Seki, N., Ozaki, T., Kato, M., Kuno, T., Nakagawa, T., Watanabe, K., Miyazaki, K., Ohira, M., Hayashi, S., et al. (2002). Identification of the p33(ING1)-regulated genes that include cyclin B1 and proto-oncogene DEK by using cDNA microarray in a mouse mammary epithelial cell line NMuMG. Cancer Res. *62*, 2203–2209.

Ueda, K. (2001). Detection of the retinoic acid-regulated genes in a RTBM1 neuroblastoma cell line using cDNA microarray. Kurume Med. J. *48*, 159–164.

van 't Veer, L.J., Dai, H., van de Vijver, M.J., He, Y.D., Hart, A.A., Mao, M., Peterse, H.L., van der Kooy, K., Marton, M.J., Witteveen, A.T., et al. (2002). Gene expression profiling predicts clinical outcome of breast cancer. Nature *415*, 530–536.

Yamanaka, Y., Hamazaki, Y., Sato, Y., Ito, K., Watanabe, K., Heike, T., Nakahata, T., and Nakamura, Y. (2002). Maturational sequence of neuroblastoma revealed by molecular analysis on cDNA microarrays. Int. J. Oncol. *21*, 803–807.

Yoshikawa, T., Nagasugi, Y., Azuma, T., Kato, M., Sugano, S., Hashimoto, K., Masuho, Y., Muramatsu, M., and Seki, N. (2000). Isolation of novel mouse genes differentially expressed in brain using cDNA microarray. Biochem. Biophys. Res. Commun. *275*, 532–537.

Accession numbers

Microarray data are available at NCBI Gene Expression Omnibus (accession number GSE2283).

American Journal of Pathology, Vol. 167, No. 1, July 2005

Tumorigenesis and Neoplastic Progression

Biological Role of Anaplastic Lymphoma Kinase in Neuroblastoma

Yuko Osajima-Hakomori,*¶‖ Izumi Miyake,*† Miki Ohira,‡ Akira Nakagawara,‡ Atsuko Nakagawa,§ and Ryuichi Sakai*

From the Growth Factor Division, National Cancer Center Research Institute, Chuo-ku, Tokyo; St. Marianna University School of Medicine,¶ Kawasaki-shi, Kanagawa; Tokyo Metropolitan Geriatric Hospital,‖ Itabashi-ku, Tokyo; the Department of Pediatrics,† Kitasato University School of Medicine, Sagamihara-shi, Kanagawa; the Division of Biochemistry,‡ Chiba Cancer Center Research Institute, Cyuo-ku, Chiba; and the Department of Pathology,§ Aichi Medical University, Aichi-gun, Aichi, Japan*

Anaplastic lymphoma kinase (ALK) is a tyrosine kinase receptor originally identified as part of the chimeric nucleophosmin-ALK protein in the t(2;5) chromosomal rearrangement associated with anaplastic large cell lymphoma. We recently demonstrated that the ALK kinase is constitutively activated by gene amplification at the ALK locus in several neuroblastoma cell lines. Forming a stable complex with hyperphosphorylated ShcC, activated ALK modifies the responsiveness of the mitogen-activated protein kinase pathway to growth factors. In the present study, the biological role of activated ALK was examined by suppressing the expression of ALK kinase in neuroblastoma cell lines using an RNA interference technique. The suppression of activated ALK in neuroblastoma cells by RNA interference significantly reduced the phosphorylation of ShcC, mitogen-activated protein kinases, and Akt, inducing rapid apoptosis in the cells. By immunohistochemical analysis, the cytoplasmic expression of ALK was detected in most of the samples of neuroblastoma tissues regardless of the stage of the tumor, whereas significant amplification of ALK was observed in only 1 of 85 cases of human neuroblastoma samples. These data demonstrate the limited frequency of ALK activation in the real progression of neuroblastoma. *(Am J Pathol 2005, 167:213–222)*

Receptor tyrosine kinases (RTKs) play an important role in regulating diverse cellular processes, such as proliferation, differentiation, survival, motility, and malignant transformation. The activation of RTKs typically requires ligand-induced receptor oligomerization, which results in tyrosine autophosphorylation of the receptors at tyrosine residues.[1–3] By recruiting specific sets of signal transducer molecules in a phosphorylation-dependent manner, each RTK is capable of inducing individual, specific cellular responses.[4] On the other hand, activation of RTKs by either mutations or overexpression is frequently found in various human malignancies.[3,5]

Anaplastic lymphoma kinase (ALK) is a 200-kd tyrosine kinase encoded by the *ALK* gene on chromosome 2p23. ALK was first identified as part of an oncogenic fusion tyrosine kinase, nucleophosmin-ALK, which is associated with anaplastic large cell lymphoma.[6,7] It was also found as a form of fusion protein with a clathrin heavy chain (CTCL) in myofibroblastic tumors.[8] Full-length ALK has the typical structure of an RTK, with a large extracellular domain, a lipophilic transmembrane segment, and a cytoplasmic tyrosine kinase domain.[9,10] ALK is highly homologous to leukocyte tyrosine kinase (LTK) and is further classified into the insulin receptor superfamily. The *LTK* gene is mainly expressed in pre-B lymphocytes and neuronal tissues,[11–13] whereas expression of the normal *ALK* gene in hematopoietic tissues has not been detected. Instead, it is dominantly expressed in the neural system.[14,15] In the developing brains of mice, specific expression of *ALK* was seen in the thalamus, mid-brain, olfactory bulb, and selected cranial regions, as well as the dorsal root, the ganglia of mice,[9,10,16] suggesting a specific role in the development of the embryonic nervous system. Currently, however, the function of ALK in adult normal tissue or carcinogenesis remains an open question. Several studies have recently indicated pleiotrophin or midkine as possible ligands for ALK.[17,18] Although they appeared to induce the functional activa-

Supported by the Program for the Promotion of Fundamental Studies in Health Science of the Organization for Pharmaceutical Safety and Research of Japan. Y.O-H. is the recipient of a Research Resident Fellowship from the Foundation for Promotion of Cancer Research, Japan.

Accepted for publication March 23, 2005.

Address reprint requests to Ryuichi Sakai, M.D., Growth Factor Division, National Cancer Center Research Institute, 5-1-1 Tsukiji, Chuo-ku, Tokyo 104-0045, Japan. E-mail: rsakai@gan2.res.ncc.go.jp.

tion of ALK, it is still unclear whether these molecules are the physiological ligands of ALK.

Neuroblastoma is one of the most common pediatric tumors derived from the sympathoadrenal linage of the neural crest. Tumors found in patients under the age of 1 year are usually favorable and often show spontaneous differentiation and regression.[19] Amplification of the N-*myc* gene occurs in approximately 25% of neuroblastomas and correlates with the aggressiveness of the disease. In addition to N-*myc* gene amplification, the expression of various genes has significant correlation with the stage of and prognosis for neuroblastoma. A high level of TrkA expression is predictive of a favorable outcome,[20] whereas TrkB is highly expressed in immature neuroblastomas with N-*myc* amplification.[21] High expression of caspase-1, -3, and -8 is correlated with favorable neuroblastomas.[22,23] On the other hand, survivin, which suppresses caspase and promotes the cell survival signal, is significantly expressed,[24] and telomerase is activated[25] in unfavorable tumors. There may be a critical difference in the expression of other molecules, including RTKs, in neuroblastoma. A recent paper showed that full-length ALK is detected in almost one-half of the cell lines derived from neuroblastomas and neuroectodermal tumors.[26] We have recently shown using mass-spectrometry analysis that ALK is a major phosphoprotein associated with hyperphosphorylated ShcC in several neuroblastoma cell lines.[27] In these cells, ALK was markedly activated, and it induced the constitutive phosphorylation of ShcC and mitogen-activated protein kinase (MAPK), regardless of stimulation by epidermal growth factor (EGF) or nerve growth factor.[27] These findings strongly suggest that constitutively activated ALK kinase plays a physiological role in the development of neuroblastoma.

In this study, we investigated the biological function of the constitutively activated ALK kinase in neuroblastoma. The RNA interference (RNAi) technique using specific sets of small interfering RNA (siRNA) was induced to inhibit the *ALK* gene expression in human neuroblastoma cells with or without gene amplification of *ALK*. The effects of disrupted ALK expression on cell survival or downstream signaling, such as MAPKs or Akt pathways, are examined to understand the biological meaning of ALK amplification in neuroblastoma cells. We also performed Southern blot analysis of primary neuroblastoma tumors from 85 patients to check whether the *ALK* gene amplification was actually present in neuroblastoma tissues. Furthermore, we sought the *ALK* gene expression in human neuroblastoma tissues using immunohistochemical analysis.

Materials and Methods

Cell Culture

Cell lines of human neuroblastoma were maintained in RPMI 1640 supplemented with 10% fetal calf serum (Sigma, St. Louis, MO), penicillin, and streptomycin at 37°C in a humidified 5% CO_2 incubator.

Reverse Transcription-Polymerase Chain Reaction (RT-PCR) Analysis

Total RNA was extracted with ISOGEN (Nippongene Japan, Toyama, Japan) from NB-39-nu and SK-N-MC cells. The PCR primer pair 5′-AGGTTCTGGCTGCAGATGGT-3′ and 5′-ACATTGTTCTCTCGAGTGCAGAC-3′ corresponding to the cytoplasmic portion of human ALK was prepared. As much as 0.25 μg of total RNA was reverse transcribed and amplified with the SuperScript One-step RT-PCR with the Platinum *Taq* kit (Invitrogen Life Technologies, Carlsbad, CA) in a total volume of 50l including 2× reaction mix, 0.2 μmol/L of each primer, and 1 μl of RT/Platinum *Taq* Mix. Amplification conditions consisted of cDNA synthesis and predenaturation at 50°C for 30 minutes and 94°C for 2 minutes followed by 25 cycles at 94°C for 15 seconds, 58°C for 30 seconds, and 72°C for 45 seconds. A final amplification for 7 minutes at 72°C finished the PCR. The product was separated with 1.2% agarose gel electrophoresis and analyzed using the Quality One System (Bio-Rad, Hercules, CA).

Immunochemical Analysis of Proteins

Immunoprecipitation and immunoblotting were performed as described previously.[27] The polyclonal antibodies against the CH1 domains of ShcC (amino acids 306–371) and the anti-ALK antibody (αALK) that was against the cytoplasmic portion (amino acid 1379–1524) of human ALK were prepared as described previously.[27,28] An anti-phosphotyrosine antibody (4G10) was obtained from UBI. Anti-p44/42 MAPKs, anti-phospho-p44/42 MAPKs, anti-Akt, and anti-phospho-Akt antibodies were purchased from Cell Signaling (Beverly, MA). Anti-EGF receptor (EGFR), anti-Ret, and anti-TrkA antibodies were purchased from Santa Cruz Biotechnology (Santa Cruz, CA). *In vitro* kinase assay for ALK was performed as previously described.[27] Anti-ALK immunoprecipitates were incubated with or without Poly-Glu/Tyr as an exogenous substrate.

Immunocytostaining

For ALK/TOTO-3, immunostaining using anti-ALK antibody was performed at first, and then nuclei were stained using TOTO-3. The cells seeded on the 24-well plates were washed with phosphate-buffered saline (PBS) three times and fixed with 4% paraformaldehyde (methanol free) for 5 minutes at room temperature. The cells were rinsed with PBS twice and then permeabilized with 0.2% Triton X-100 solution in PBS for 10 minutes at room temperature. The cells were blocked with 5% goat serum and 3% bovine serum albumin–Tris-buffered saline for 30 minutes at room temperature. The blocking solution was drained off, and the cells were incubated with a 1:1000 dilution of αALK for 1 hour at room temperature. The cells were rinsed with PBS three times and incubated with a 1:2000 dilution of Alexa fluor (Molecular Probes, Eugene, OR) and 1: 100 dilution of TOTO-3 (Molecular Probes) for

Table 1. Patient Characteristics of Neuroblastoma Tissues with *ALK* Gene Gain or Amplification

Case	Age*	Primary tumor		Copy nos. of *ALK*‡	Amplification of N-*myc* (*n*)
		Location	Clinical stage†		
1	3y5m	Adrenal gland	IV	2.0 ± 0.2	+ (35)
2	5y0m	Peritoneum	IV	1.8 ± 0.1	+ (>150)
3	2y7m	Abdomen	IV	2.1 ± 0.8	+ (150)
4	8m	Adrenal gland	I	3.0 ± 1.0	−
5	4y9m	Abdomen	IV	2.0 ± 0.2	−
6	3y9m	Adrenal gland	III	2.7 ± 0.2	+ (>150)
7	1y4m	Adrenal gland	IV	2.8 ± 1.0	+ (150)
8	1y7m	Adrenal gland	IV	9.5 ± 2.2	+ (>100)

*Age of onset: year (y), month (m).
†The staging criterion was based on the International Neuroblastoma Staging System.
‡The averages of the calculated copy numbers from three independent blottings are shown.

30 minutes at room temperature. The cells were washed three times with PBS and mounted in glycerol-based 2.5% 1,4-diazabicyclo[2,2,2] octan. Confocal laser scanning analysis was carried out. For ALK/TUNEL, we first carried out TUNEL and then proceeded to standard immunocytochemistry using anti-ALK antibody. TUNEL was performed using the DeadEnd Fluorometric TUNEL System (Promega, Madison, WI) with the following modifications. The NB-39-nu cells seeded on the 24-well plates that were treated with siRNAs were washed with PBS twice and fixed with 4% paraformaldehyde (methanol free) for 25 minutes at 4°C. The cells were rinsed with PBS twice and then permeabilized with 0.2% Triton X-100 solution in PBS for 5 minutes at room temperature. The cells were washed with PBS twice and covered with an equilibration buffer (from the kit) for 10 minutes at room temperature. The equilibration buffer was drained off, and a reaction buffer containing the equilibration buffer, nucleotide mix, and terminal deoxynucleotidyl transferase enzyme was added to the cells and incubated at 37°C for 1 hour, avoiding exposure to light. The cells were incubated for 15 minutes at room temperature with 2× standard saline citrate to stop the reaction. The cells were washed with PBS three times and then stained for ALK using immunofluorescence as follows. The cells were blocked with 2% bovine serum albumin (Boehringer Mannheim, Germany) for 30 minutes at room temperature. The blocking solution was drained off, and the cells were incubated with a 1:1000 dilution of αALK for 1 hour at room temperature. The cells were rinsed with PBS three times and incubated with a 1:40 dilution of rhodamine-conjugated goat anti-rabbit secondary antibody (Santa Cruz Biotechnology) for 30 minutes at room temperature. The cells were washed three times with PBS and then mounted and observed in the same manner as that for ALK/TOTO-3.

DNA Extraction and Southern Blotting

Genomic DNAs derived from neuroblastoma cell lines were obtained from cultured cells as described using the procedure of Perucho et al.[29] Samples of 85 neuroblastoma tissues were collected at the Chiba Cancer Center and stored as forms of genomic DNA. The characteristics of some of these patients are shown in Table 1. The stage criterion was based on the International Neuroblastoma Staging System.[30] Samples of 5 μg of DNA digested by *Eco*RI were electrophoresed in 0.8% agarose gel and blotted onto nitrocellulose filters (Hybond-N+; Amersham, Piscataway, NJ). The probes for detecting the *ALK* gene, N-*myc* gene, and *ShcC* gene were used in our previous study.[27] The intensities of these signals were measured using a Molecular Imager FxPro (Bio-Rad). This study was approved by the ethical judging committee of the National Cancer Center and the Chiba Cancer Center of Japan.

RNA Interference Technique

Twenty-one-nucleotide double-stranded RNAs were synthesized and purified using Dharmacon Research (Lafayette, CO). To suppress the expression of ALK protein, two different pairs of ALK siRNAs, ALK-siRNA1 and ALK-siRNA2, were obtained. The sequences were 5′-GAGUCUGGCAGUUGACUUCdTdT-3′ for ALK-siRNA1 and 5′-GCUCCGGCGUGCCAAGCAGdTdT-3′ for ALK-siRNA2, corresponding to coding region 153 to 171 and 399 to 417 relative to the first nucleotide of the start codon, respectively. Entire sequences were derived from the sequence of human *ALK* mRNA (accession no. HSU62540). An siRNA, targeting a sequence in the firefly (*Photinus pyralis*) luciferase mRNA, was used as a negative control (Dharmacon) (luc-siRNA). We also used a scramble siRNA, Scramble Duplex II (Dharmacon) (s-siRNA) as a mismatch siRNA control in addition to luc-siRNA.

NB-39-nu cells were trypsinized, diluted with growth medium containing 10% fetal calf serum, and transferred to 12-well plates at 6×10^4 cells per well for 24 hours before transfection. The transfection of siRNA was carried out using jetSI (Poly plus transfection). A total of 100 μl of serum-free growth medium and 4 μl of jetSI per well were preincubated for 5 to 10 minutes at room temperature. While the incubation was being performed, 100 μl of serum-free growth medium was mixed with 5 μl of 20 μmol/L siRNA duplex (100 pmol). Total siRNA amounts of 50, 100, and 200 pmol were checked in preliminary experiments to find out 100 pmol is the minimal and optimal amount in this scale of RNAi. The 100 μl of jetSI serum-free medium solution was added to the 100 μl of siRNA

duplex solution, gently mixed, and incubated for 30 minutes at room temperature. The growth medium on the cells was removed, and 800 μl of serum-free medium was added to each well. A total of 200 μl of the entire mixture was overlaid onto the cells, and cells were incubated for 4 hours at 37°C in a 5% CO_2 incubator. After incubation, 1 ml of medium containing 4% fetal calf serum was added without removing the transfection mixture (final concentration 2%). The cells were assayed 84 hours after transfection. SK-N-MC cells were seeded in 12-well plates at a concentration of 1.3×10^5 cells per well. These were treated with siRNAs in the same way as NB-39-nu and assayed 48 hours after transfection. In the 24-well plate, the cells were seeded at the same concentration as the 12-well plate, and siRNAs and all other reagents were used at half volume. After transfection, the cells were examined under a light microscope every day.

Double Staining for ALK and TUNEL

For double staining, we first carried out TUNEL and then proceeded to standard immunocytochemistry using anti-ALK antibody. TUNEL was performed using the DeadEnd Fluorometric TUNEL System (Promega) with the following modifications. The NB-39-nu cells seeded on the 24-well plates that were treated with siRNAs were washed with PBS twice and fixed with 4% paraformaldehyde (methanol free) for 25 minutes at 4°C. The cells were rinsed with PBS twice and then permeabilized with 0.2% Triton X-100 solution in PBS for 5 minutes at room temperature. The cells were washed with PBS twice and covered with an equilibration buffer (from the kit) for 10 minutes at room temperature. The equilibration buffer was drained off, and a reaction buffer containing the equilibration buffer, nucleotide mix, and terminal deoxynucleotidyl transferase enzyme was added to the cells and incubated at 37°C for 1 hour, avoiding exposure to light. The cells were incubated for 15 minutes at room temperature with 2× standard saline citrate to stop the reaction. The cells were washed with PBS three times and then stained for ALK using immunofluorescence as follows. The cells were blocked with 2% bovine serum albumin (Boehringer Mannheim) for 30 minutes at room temperature. The blocking solution was drained off, and the cells were incubated with a 1:1000 dilution of αALK for 1 hour at room temperature. The cells were rinsed with PBS three times and incubated with a 1:40 dilution of rhodamine-conjugated goat anti-rabbit secondary antibody (Santa Cruz Biotechnology) for 30 minutes at room temperature. The cells were washed three times with PBS and mounted in glycerol-based 2.5% 1,4-diazabicyclo[2,2,2] octan. Confocal laser scanning analysis was carried out.

DNA Fragmentation Assay

To detect apoptotic DNA cleavage, DNA fragmentation assay was performed using an Apoptotic DNA Ladder kit (Chemicon International, Inc., Temecula, CA). The cells seeded on the 12-well plates that were treated with siRNAs as previously mentioned were collected in 1.5-ml microcentrifuge tubes. The cells were washed with PBS, centrifuged, and lysed with 20 μl of TE lysis buffer. The lysates were incubated with 5 μl of enzyme A (RNase A) at 37°C for 10 minutes and then at 55°C for 30 minutes after the addition of 5 μl of Enzyme B (Proteinase K). Afterward, 5 μl of ammonium acetate solution and 100 μl of absolute ethanol were added, and the samples were kept at −20°C for 10 minutes. The samples were centrifuged, and the pellets were washed with 70% ethanol. Then the DNA pellets were dissolved in 30 μl of DNA suspension buffer. DNA fragmentations were visualized by electrophoresis on 2% agarose gel containing ethidium bromide.

Immunohistochemistry

As for positive control, tumor xenograft was made by injection of NB-39-nu cells subcutaneously in 5-week-old SCID mice. Immunohistochemical staining with ALK antibody (αALK) (1:1000), was performed on 16 human neuroblastoma tumors selected from the surgical pathology file at the Department of Pathology, Aichi Medical University based on the results of histopathology evaluation[31] and N-*myc* status. All of those tumor samples were obtained before chemotherapy and irradiation therapy and included nine favorable histology cases with nonamplified N-*myc* (FH&NA), two unfavorable histology cases with amplified N-*myc* (UH&A), and five unfavorable histology cases with nonamplified N-*myc* (UH&NA).

Four-micrometer-thick sections from the formalin-fixed and paraffin-embedded tissue samples were deparaffinized and microwaved for three times for 5 minutes in Na-citrate buffer (pH 6.0) for antigen retrieval. The slides were first immersed in 0.3% hydrogen peroxide in methanol for 20 minutes and then in 10% normal goat serum for 30 minutes. The primary antibody (αALK) was then applied at 4°C overnight, followed by a standard staining procedure using the Vectastain ABC kit (Vector Laboratories, Burlingame, CA). Sections were counterstained with hematoxylin for light microscopic review and evaluation. ALK was always positively detected in the cytoplasm of NB-39-nu tumor xenograft and in the cytoplasm and neuritic processes of normal ganglion cells in the separate positive control sections as well as in the test sections as built-in control, whenever available. As for the negative controls, normal rabbit immunoglobulins (1:500 dilution; Vector Laboratories) or preimmune serum for α ALK (1:1000 dilution) was applied as the primary antibody.

Results

Significant Amplification of the ALK Gene and Constitutive Activation of ALK Kinase in Three Neuroblastoma Cell Lines

As shown in Figure 1A, NB-39-nu, Nagai, and NB-1 cells have significant levels of amplification of the *ALK* gene (30–40 copies per cell) among 25 neuroblastoma and neuroepithelioma cell lines examined. Other cell lines such as SK-N-MC have only one copy of the *ALK* gene just like the

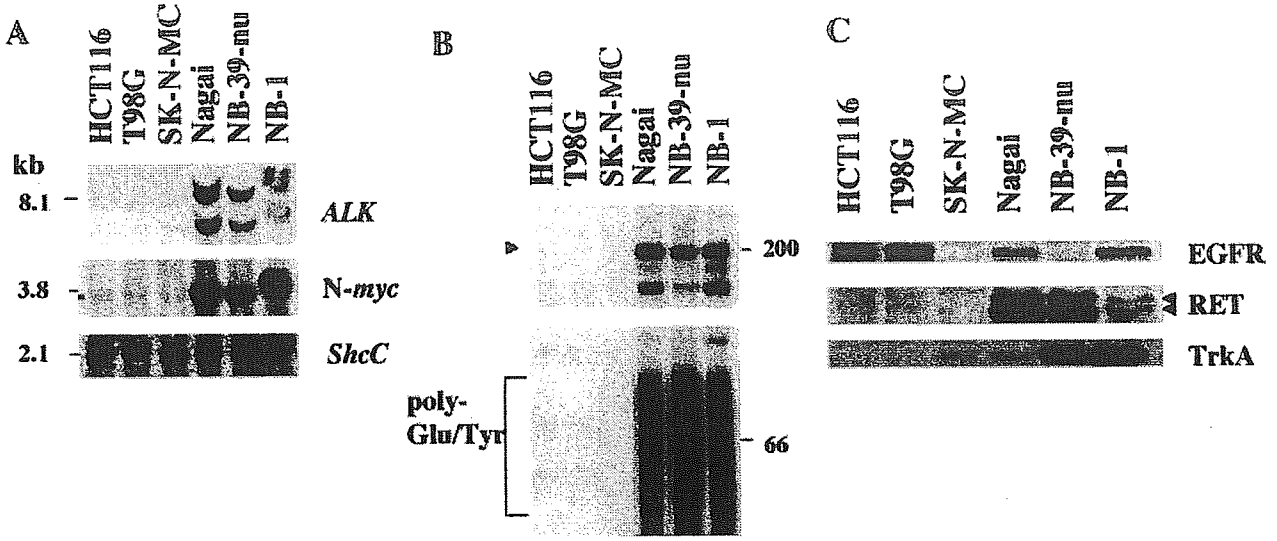

Figure 1. Marked gene amplification of the *ALK* locus and significant elevation of kinase activity of ALK in NB-39-nu, Nagai, and NB-1 cells. **A:** To detect ALK gene amplification, samples of 10 μg of DNA were digested with *Eco*RI. Fragments of about 2.5, 3.1, 6.1, and 8.1 kb were detected using the ^{32}P-labeled probe prepared as previously described.[27] Amplification of the N-*myc* gene was detected using the same filter re-hybridized with the probe for N-*myc*. As a control for the amounts of DNA, the same filter was re-hybridized with the probe for *ShcC*. **B:** *In vitro* kinase assay of ALK in neuroblastoma cells immunoprecipitated with αALK was performed as previously described.[27] Kinase reaction was performed without (**top panel**) or with (**bottom panel**) poly-Glu/Tyr (4:1) as exogenous substrates. Autophosphorylated ALK protein is marked by an **arrow**. Phosphorylated poly-Glu/Tyr is detected as smear indicated by the bracket. **C:** The expression patterns of other receptor tyrosine kinases in neuroblastoma cell lines. Each cell line was harvested, and about 30 μg of whole-cell lysates was subjected to Western blot analysis using the antibodies as indicated on the right. RET proteins are marked by **arrows**.

other types of solid tumor cell lines used as controls. *In vitro* kinase assay revealed outstanding ALK kinase activity in these three cell lines compared with other cells (Figure 1B), which is consistent with our previous study.[27] To examine whether overexpressed and activated ALK affects the expression of other RTKs in these cells, protein expression levels of RTKs, including EGFR, Ret, and TrkA, are compared with other cell lines. Significantly high levels of expression of EGFR and TrkA were observed in two of three cell lines overexpressing ALK (Figure 1C, top and bottom). Ret expression was commonly elevated in all three cell lines with activated ALK, especially in Nagai and NB-39-nu (Figure 1C, middle), consistent with previous study by Northern blotting.[32] Although it is unknown whether overexpression of these RTKs is related to overexpression of ALK, no obvious down-regulation of other RTKs was found in these *ALK*-amplified cell lines.

Inhibition of Activated ShcC, MAPKs, and Akt by Suppressing Activated ALK

To investigate the effect of suppressing the ALK expression level in *ALK*-amplified neuroblastoma cells using the RNAi technique, we synthesized two different RNA duplexes directed against nucleotide positions 153 to 171 and 399 to 417 within coding region *ALK* cDNA (ALK-siRNA1 and ALK-siRNA2, respectively). Because cotransfection of ALK-siRNA1 and ALK-siRNA2 was very effective in suppressing ALK expression, we performed all experiments presented here using a combination of two siRNAs, although similar results were obtained using only ALK-siRNA2. A sequence against the firefly luciferase gene (luc-siRNA) was used as a negative control. The expression of ALK protein is remarkably elevated in NB-39-nu and Nagai compared with other neuroblastoma cell lines, such as SK-M-MC (Figure 2A), caused by gene amplification.[27] The RNA duplexes were transfected into NB-39-nu cells with *ALK* gene amplification and SK-N-MC cells containing only a single copy of the *ALK* gene. We also tried to introduce ALK-siRNAs in several different neuroblastoma cell lines with or without *ALK* amplification in addition to NB-39-nu and SK-N-MC cells, resulting in partial or no reduction of ALK expression presumably due to the unsuccessful introduction in those cells. Therefore, we decided to use these two cell lines to perform further analysis of the effect of ALK knockdown by RNAi technique. RT-PCR analysis revealed that ALK mRNA level was reduced in both NB-39-nu cells and SK-N-MC cells treated with ALK-siRNAs, not in the cells treated with luc-siRNA and s-siRNA (Figure 2B). Both expression and phosphorylation of ALK kinase were significantly suppressed in the NB-39-nu cells treated with ALK-siRNAs compared with a mock-transfection control or cells treated with luc-siRNA (Figure 2C). In these cells, phosphorylation of ShcC was also suppressed despite the unchanged total amount of ShcC (Figure 2C), demonstrating that ShcC is a potent substrate of activated ALK kinase and that activation of ALK is actually responsible for the hyperphosphorylation of ShcC in these cancer cells. While the expression of downstream molecules, such as p44/42 MAPKs and Akt, was not affected by ALK-siRNAs, phosphorylation of these molecules was markedly reduced (Figure 2C). These results suggest that the Ras-MAPK pathway and the phosphatidylinositol 3-kinase/Akt pathway are dominantly regulated by activated ALK kinase in these cells. Interestingly, in SK-N-MC cells treated with ALK-siRNAs, phosphorylation levels of ShcC, p44/42 MAPKs, and Akt were not affected by

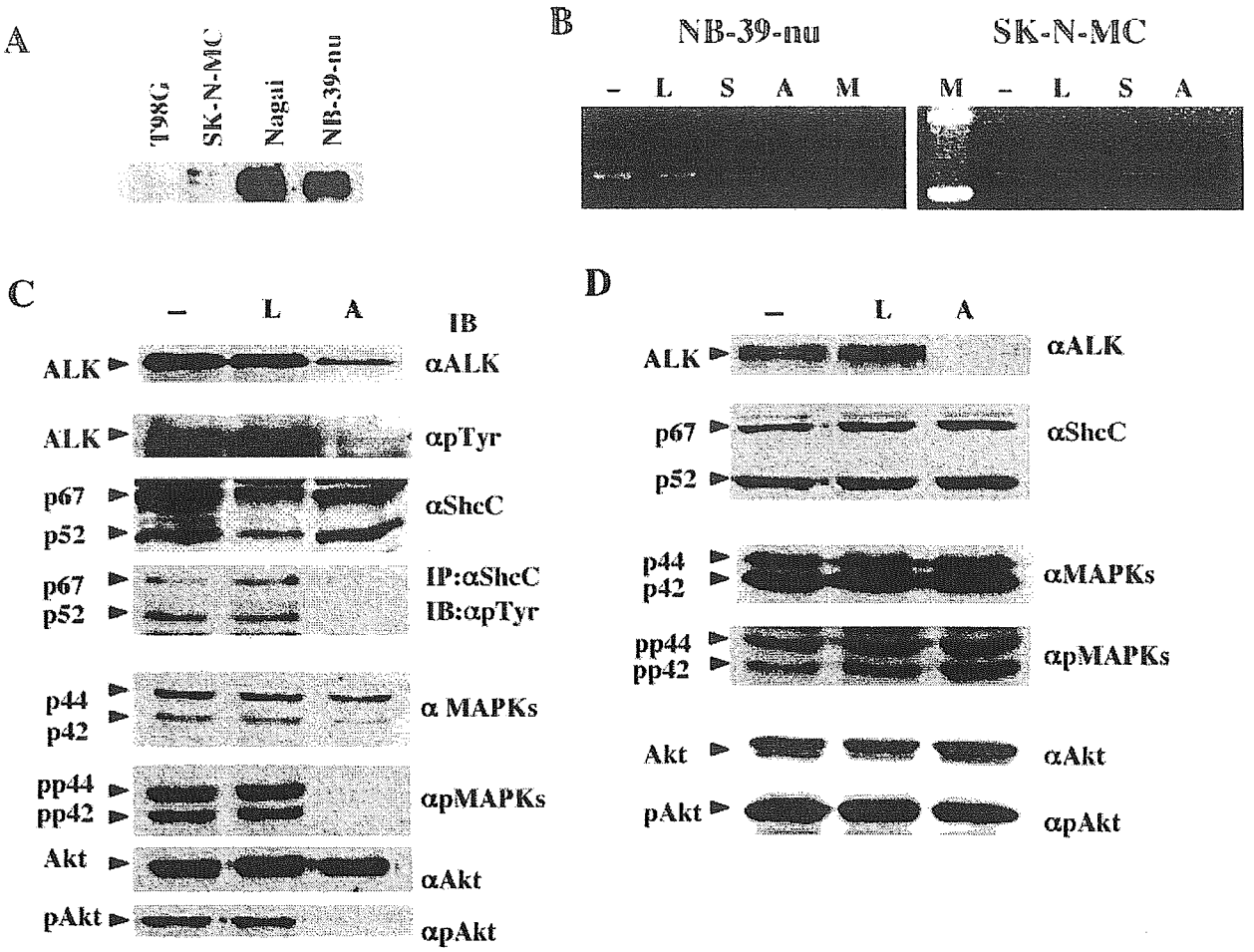

Figure 2. Suppression of ALK expression by siRNAs and changes in downstream molecules NB-39-nu cells and SK-N-MC cells. **A:** Expression levels of ALK protein in neuroblastoma cell lines including NB-39-nu and SK-N-MC. Each cell line was harvested, and about 30 μg of whole-cell lysates was subjected to Western blot analysis using αALK. **B:** mRNA levels of *Alk* in NB-39-nu cells. The cells were lysed at 84 hours after transfection and analyzed by RT-PCR. –, mock transfection; L, cells treated with luc-siRNA; S, cells treated with s-siRNA; A, cells treated with ALK-siRNAs; M, marker. **C:** NB-39-nu cells were harvested 84 hours after transfection. About 10 μg of whole-cell lysates or 250 μg of lysates immunoprecipitated with αShcC was subjected to Western blot analysis using the antibodies as indicated on the right. –, mock transfection; L, cells treated with luc-siRNA; A, cells treated with ALK-siRNAs. **D:** SK-N-MC cells were harvested 48 hours after transfection. About 10 μg of whole-cell lysates was subjected to Western blot analysis using the antibodies as indicated on the right. Bands of ShcC are marked by **arrows**. –, mock transfection; L, cells treated with luc-siRNA; A, cells treated with ALK-siRNAs.

ALK-siRNAs despite further suppression of the basal ALK expression level (Figure 2D), indicating that these pathways are not under the control of ALK in SK-N-MC cells.

Induction of Apoptosis by Suppression of Activated ALK

At 84 hours after transfection, apoptotic morphological changes, such as cell rounding, cytoplasmic blebbing, and irregularities of shape, were observed in NB-39-nu cells treated with ALK-siRNAs, whereas no significant changes were seen in the mock-transfected cells or in the luc-siRNA and the s-siRNA treated cells (Figure 3A). These morphological changes were not observed in SK-N-MC cells treated with ALK-siRNAs (data not shown). At 90 hours after transfection, NB-39-nu cells treated with ALK-siRNAs started to detach from the dish due to cell death.

To examine the localization of expression of ALK kinase, we performed double staining by anti-ALK antibody and TOTO-3, which stains the nucleus, in several neuroblastic cell lines. As shown in Figure 1D, unexpectedly, ALK protein overexpressed in NB-39-nu cells is localized in both membrane and cytoplasm. ALK staining was very weak in cell lines such as YT-nu and SK-N-MC with one copy of the *ALK* gene, however, its localization appeared to be the same as in NB-39-nu (data not shown). It was observed that the expression of ALK was completely lost after the RNAi-induced suppression of ALK (Figure 3C, top). To confirm whether the cell death resulted from apoptosis, cells were also analyzed by immunofluorescent TUNEL staining in NB-39-nu cells. TUNEL staining was clearly positive in these cells at 84 hours after transfection (Figure 3C, middle), indicating that apoptosis was induced in NB-39-nu cells treated with ALK-siRNAs. No significant TUNEL staining was observed in the mock-transfected cells or the luc-siRNA treated cells. Finally, DNA fragmentation assay was performed to measure the endonuclease activity accompa-

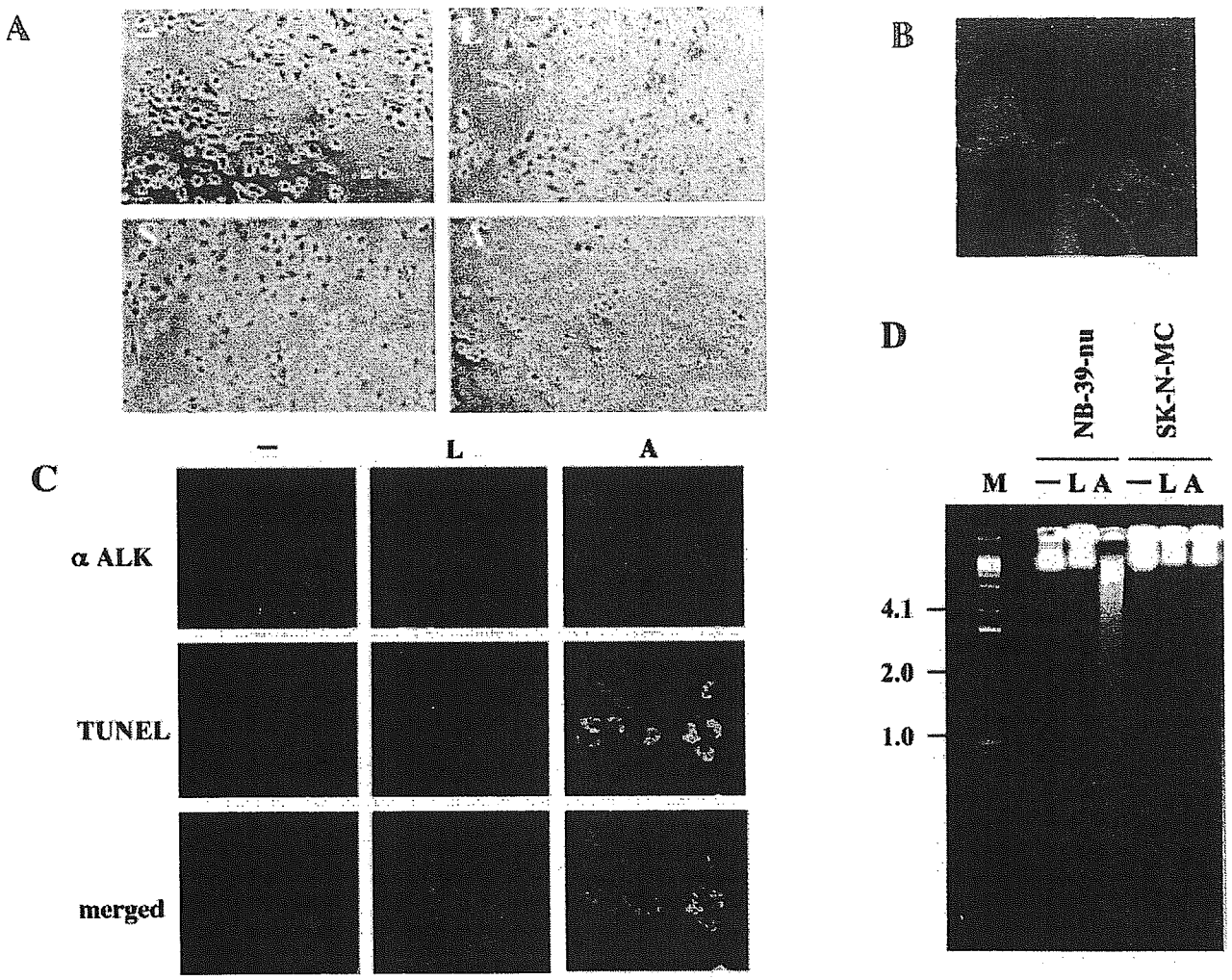

Figure 3. Induction of apoptosis in NB-39-nu cells treated with ALK-siRNAs. **A:** NB-39-nu cells on the dish were observed 84 hours after transfection under a light microscope. −, mock transfection; L, cells treated with luc-siRNA; S, cells treated with s-siRNA; A, cells treated with ALK-siRNAs. **B:** Cytoplasmic expression of ALK by immunocytostaining. The cells were stained for the expression of ALK (red) and apoptotic cells by TOTO-3 (blue). **C:** Cells on 24-well plates were fixed, and TUNEL assay was followed by staining with αALK (GST). The cells were stained for the expression of ALK (red) and apoptotic cells by TUNEL (green). −, mock transfection; L, cells treated with luc-siRNA; A, cells treated with ALK-siRNAs. **D:** DNA fragmentation assay in NB-39-nu cells and SK-N-MC cells treated with siRNAs. Genomic DNA was extracted 84 hours and 48 hours after transfection in NB-39-nu and in SK-N-MC, respectively. They were analyzed using electrophoresis. −, mock transfection; L, cells treated with luc-siRNA; A, cells treated with ALK-siRNAs; M, marker.

nied by apoptosis. The formation of significant DNA fragmentation was observed in the NB-39-nu cells but not in SK-N-MC cells treated with ALK-siRNAs (Figure 3D), indicating that cell apoptosis was induced through the suppression of ALK only in the NB-39-nu cells. This suggests that signaling pathways downstream of activated ALK dominantly regulate the survival of neuroblastoma cells with amplified ALK; therefore, the loss of ALK protein results in apoptotic changes to these cells.

Expression of ALK in Primary Neuroblastoma Tissues

Immunohistochemically, ALK was positively detected both in the cytoplasm of the neuroblastic cells and in the fine meshwork of neuropil of seven of nine tumors with favorable histology cases with nonamplified *N-myc* (FH&NA) (Figure 4, B and C). All seven unfavorable histology tumors (two UH&A tumors and five UH&NA tumors) were positive in the cytoplasm and/or in the fine meshwork of neuropil for ALK (Figure 4A). There was no correlation between the frequency or intensity of ALK-staining and histology of neuroblastoma tissues, showing majority of neuroblastoma samples showed a detectable amount of ALK. There was no significant staining using preimmune serum from the same rabbit as that for anti-ALK antibody (data not shown). Essentially the same results were obtained using a mouse monoclonal antibody against human ALK (ALK1: DAKO) (data not shown).

Amplification of the ALK Gene in Primary Neuroblastoma Tissues

It is essential to show whether ALK overexpression or gene amplification occurs in actual human neuroblastoma tissues in addition to neuroblastoma cell lines.

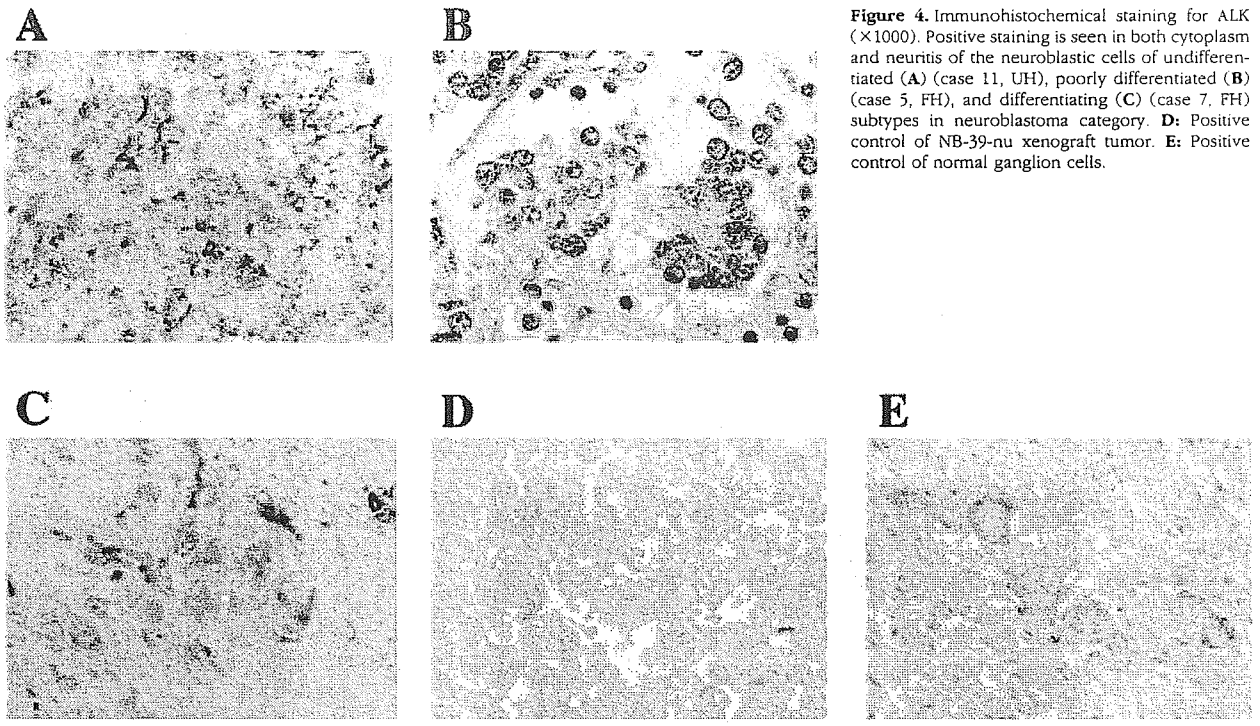

Figure 4. Immunohistochemical staining for ALK (×1000). Positive staining is seen in both cytoplasm and neuritis of the neuroblastic cells of undifferentiated (**A**) (case 11, UH), poorly differentiated (**B**) (case 5, FH), and differentiating (**C**) (case 7, FH) subtypes in neuroblastoma category. **D:** Positive control of NB-39-nu xenograft tumor. **E:** Positive control of normal ganglion cells.

Therefore, the mRNA amount of ALK kinase was first examined by RT-PCR on 32 primary neuroblastoma tissues (16 tissues with N-*myc* amplification and 16 tissues without N-*myc* amplification). Two of 32 cases showed slight elevation of *ALK* mRNA expression using several primer sets beyond the average expression level (data not shown).

To obtain more precise information about the copy numbers of *ALK*, we next analyzed the genomic DNAs of primary neuroblastoma tissues using Southern blot analysis. Whole purified DNA samples of tumors from 85 patients were examined. About the same number of N-*myc*-positive and N-*myc*-negative samples were collected to examine the relation between *Alk* and N-*myc* amplification. The intensities of signals on Southern blot membranes corresponding to the *ALK* gene and control *ShcC* gene, which is located on 9q22, were measured using a Molecular Imager FxPro (Bio-Rad), and the ratio of *ALK* signals to *ShcC* signals was calculated for each sample. Because more than 80% (70 samples) showed consistent ratios with each other in each experiment, these samples are treated as putative "single copy" controls. As several other samples showed apparently elevated intensity ratios, suggesting *ALK* amplification, relative copy numbers of *ALK* were calculated in comparison with average intensity ratios of putative single copy controls in each experiment. The results showed that there was significant *ALK* gene amplification in 8 of 85 patients (9.4%) (Figure 5). Seven of these eight cases, however, had only 1.8 to 3.0 copies of the *ALK* gene, suggesting a moderate gain of chromosomal focus rather than severe amplification. There was only one case that had outstanding amplification of ALK with approximately 10 copies. N-*myc* gene amplification was also detected in this case. The characteristics of the eight patients with *ALK* gain or amplification are shown in Table 1. Whereas seven of eight patients were classified as Stage III or IV (one as Stage III and six as Stage IV), the rest was classified as Stage I. The case with *ALK* amplification had N-*myc* amplification and was classified as Stage IV. Seven of eight patients were more than 1 year of age.

Discussion

Studies on ALK kinase demonstrate that activated ALK is involved in malignant tumor formation as forms of fusion proteins that force oligomerization of this kinase. We recently showed that the intact form of ALK protein is con-

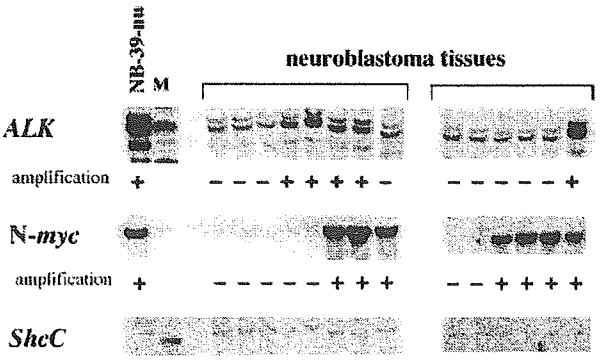

Figure 5. Detection of gene amplification of *ALK* and N-*myc* in primary neuroblastoma tissues. *ALK* was amplified in eight cases, and five of these eight cases are shown. The probe for *ALK* was removed from the filters, and the filters were re-hybridized in turn with other probes. Of eight cases with *ALK* amplification, N-*myc* amplification was detected in six cases and not detected in two cases. The probe for *ShcC* was used as a control for the amounts of DNA. M, marker.

stitutively activated by *ALK* gene amplification in three neuroblastoma cell lines, indicating a novel mechanism of activation of ALK kinase in malignancies.[27] In this study, amplification of the *ALK* gene was detected in primary neuroblastoma tissues for the first time. This suggests that activated ALK kinase plays a real role in the pathophysiology of neuroblastoma, such as giving a more malignant phenotype to the tumors by perturbing signal transduction. Recently, Motegi et al[33] showed that ALK transmits both mitogenic and differentiation signals, and that the MAPK pathway plays an important role in these effects in SK-N-SH cells without *ALK* gene amplification. Together with the fact that activated ALK surpasses regulation by other RTKs in cell lines with *ALK* gene amplification,[27] our new results showing apoptotic changes caused by the suppression of activated ALK protein clearly demonstrate the dominant role of ALK kinase in the survival of the *ALK*-amplified type of neuroblastoma.

The frequency and copy numbers of gene amplification of ALK were significantly lower in neuroblastic tumors compared with neuroblastic cell lines. Remarkable amplification of the *ALK* gene was detected in 1 tumor tissue of 85 tumor samples examined. Three neuroblastoma cell lines with *ALK* amplification had more than 30 copies of *ALK*, whereas primary neuroblastoma containing *ALK* gene amplification had within a range of 2 to 10 copies. This may be due to underestimation of the copy number in the tumor cells because of contamination of stromal cells and lymphocytes into the tumor tissues.[34,35] There may also be a mechanism in which cells with a higher copy number of *ALK* become the major population during the establishment of cell lines because of their growth advantage. Immunohistochemical analysis demonstrated, however, universal cytoplasmic expression of ALK in a wide range of neuroblastoma tumor samples, suggesting some transcriptional or posttranslational regulation of the ALK amount might exist in neuroblastoma cells. Although, due to the condition of the samples, we were unable to obtain information on the copy numbers of the *ALK* gene as for the samples used in the immunohistochemical analysis, further immunohistochemical screening may reveal neuroblastoma tissues with an outstanding amount of ALK protein because of gene amplification.

The N-*myc* gene was also amplified in this tumor and in all three cell lines with *ALK* amplification (NB-39-nu, Nagai, and NB-1). N-*myc* is located on 2p24.3 and *ALK* is on 2p23.2, suggesting that there is a tendency to synchronic amplification between N-*myc* and *ALK*. We were unable to conclude that there was an association between ALK amplification and prognosis mainly due to the limited number of positive samples and the short-term follow-up. Moreover, the *ALK* gene locus appears too far from the N-*myc* gene locus to be within a single amplicon. Further analysis in a greater number of samples with longer follow-up is necessary.

The activation of ALK results in hyperphosphorylation of ShcC in neuroblastoma cells, and NB-39-nu cells treated with ALK-siRNAs show suppressed tyrosine phosphorylation of ShcC, followed by apoptotic changes to these cells, suggesting that ShcC is a physiological substrate of the activated ALK kinase and that the ALK-ShcC pathway dominantly controls the survival of NB-39-nu cells even with the existence of other RTKs, such as EGFR, TrkA, and Ret. In neuronal cells, both ShcB (Sli/SCK) and ShcC (Rai/N-Shc) can bind activated RTKs, including the EGFR and Trk receptor.[36–39] Mice lacking both ShcB and ShcC exhibit a significant loss of sympathetic neurons, suggesting that ShcB and ShcC act in supporting sympathetic development and survival.[28] A recent study also showed that ShcC is a physiological substrate of Ret kinase and that it exerts a prosurvival function in neuronal cells.[40] Although high levels of TrkA expression correlate with a favorable outcome of neuroblastoma patients,[20] TrkA expression was significantly high in NB-39-nu and Nagai, which derive from tumors with a poor prognosis. This discrepancy may also be explained by the overwhelming control of cell survival by ALK kinase in these cell lines. Neuronal apoptosis is regulated through the action of critical protein kinase cascades, such as the phosphatidylinositol 3-kinase/Akt pathway and the Ras-MAPK pathway.[41,42] Apparently, neither pathway is properly controlled by EGF or nerve growth factor in NB-39-nu cells or Nagai cells.[27] Here, we also demonstrated that the suppression of activated ALK blocks MAPKs and Akt in these cells, resulting in apoptosis. On the other hand, the activity of MAPKs and Akt was not reduced by the suppression of a single copy of *ALK* in SK-N-MC cells. These results suggest that activation of ALK kinase completely remodeled the cellular signaling transduction pathways through ShcC so that cell survival entirely depended on signals originating from ALK kinase.

In conclusion, phosphorylation of several signaling molecules and cancer survival might be under the control of activated ALK kinase when gene amplification of ALK is as significant as in NB-39-nu cells, although the frequency of gene amplification in neuroblastoma tissues is not high. Cytoplasmic expression of ALK in neuroblastoma cells may suggest distinct function of this kinase in cell proliferation and survival. These findings further suggest that activated ALK kinase will be indispensable information for prognosis and treatment of neuroblastoma although the frequency is low.

References

1. Ullrich A, Schlessinger J: Signal transduction by receptors with tyrosine kinase activity. Cell 1990, 61:203–212
2. Heldin CH: Dimerization of cell surface receptors in signal transduction. Cell 1995, 80:213–223
3. Blume-Jensen P, Hunter T: Oncogenic kinase signalling. Nature 2001, 411:355–365
4. Pawson T: Protein modules and signalling networks. Nature 1995, 373:573–580
5. Kozlowski M, Larose L, Lee F, Le DM, Rottapel R, Siminovitch KA: SHP-1 binds and negatively modulates the c-Kit receptor by interaction with tyrosine 569 in the c-Kit juxtamembrane domain. Mol Cell Biol 1998, 18:2089–2099
6. Morris SW, Kirstein MN, Valentine MB, Dittmer KG, Shapiro DN, Saltman DL, Look AT: Fusion of a kinase gene ALK, to a nucleolar protein gene NPM, in non-Hodgkin's lymphoma. Science 1994, 263:1281–1284

7. Shiota M, Fujimoto J, Semba T, Satoh H, Yamamoto T, Mori S: Hyperphosphorylation of a novel 80 kDa protein-tyrosine kinase similar to Ltk in a human Ki-1 lymphoma cell line, AMS3. Oncogene 1994, 9:1567–1574
8. Bridge JA, Kanamori M, Ma Z, Pickering D, Hill DA, Lydiatt W, Lui MY, Colleoni GW, Antonescu CR, Ladanyi M, Morris SW: Fusion of the ALK gene to the clathrin heavy chain gene, CLTC, in inflammatory myofibroblastic tumor. Am J Pathol 2001, 159:411–415
9. Iwahara T, Fujimoto J, Wen D, Cupples R, Bucay N, Arakawa T, Mori S, Ratzkin B, Yamamoto T: Molecular characterization of ALK, a receptor tyrosine kinase expressed specifically in the nervous system. Oncogene 1997, 14:439–449
10. Morris SW, Naeve C, Mathew P, James PL, Kirstein MN, Cui X, Witte DP: ALK, the chromosome 2 gene locus altered by the t(2;5) in non-Hodgkin's lymphoma, encodes a novel neural receptor tyrosine kinase that is highly related to leukocyte tyrosine kinase (LTK). Oncogene 1997, 14:2175–2188
11. Ben-Neriah Y, Bauskin AR: Leukocytes express a novel gene encoding a putative transmembrane protein-kinase devoid of an extracellular domain. Nature 1988, 333:672–676
12. Maru Y, Hirai H, Takaku F: Human Itk: gene structure and preferential expression in human leukemic cells. Oncogene Res 1990, 5:199–204
13. Bernards A, de la Monte SM: The Itk receptor tyrosine kinase is expressed in pre-B lymphocytes and cerebral neurons and uses a non-AUG translational initiator. EMBO J 1990, 9:2279–2287
14. Pulford K, Lamant L, Morris SW, Butler LH, Wood KM, Stroud D, Delsol G, Mason DY: Detection of anaplastic lymphoma kinase (ALK) and nucleolar protein nucleophosmin (NPM)-ALK proteins in normal and neoplastic cells with the monoclonal antibody ALK1. Blood 1997, 89:1394–1404
15. Shiota M, Fujimoto J, Takenaga M, Satoh H, Ichinohasama R, Abe M, Nakano M, Yamamoto T, Mori S: Diagnosis of t(2;5)(p23;q35)-associated Ki-1 lymphoma with immunohistochemistry. Blood 1994, 84:3648–3652
16. Duyster J, Bai RY, Morris SW: Translocations involving anaplastic lymphoma kinase (ALK). Oncogene 2001, 20:5623–5637
17. Stoica GE, Kuo A, Aigner A, Sunitha I, Souttou B, Malerczyk C, Caughey DJ, Wen D, Karavanov A, Riegel AT, Wellstein A: Identification of anaplastic lymphoma kinase as a receptor for the growth factor pleiotrophin. J Biol Chem 2001, 276:16772–16779
18. Stoica GE, Kuo A, Powers C, Bowden ET, Sale EB, Riegel AT, Wellstein A: Midkine binds to anaplastic lymphoma kinase (ALK) and acts as a growth factor for different cell types. J Biol Chem 2002, 277:35990–35998
19. Evans AE, D'Angio GJ, Randolph J: A proposed staging for children with neuroblastoma: children's cancer study group A. Cancer 1971, 27:374–378
20. Nakagawara A, Arima-Nakagawara M, Scavarda NJ, Azar CG, Cantor AB, Brodeur GM: Association between high levels of expression of the TRK gene and favorable outcome in human neuroblastoma. N Engl J Med 1993, 328:847–854
21. Nakagawara A, Azar CG, Scavarda NJ, Brodeur GM: Expression and function of TRK-B and BDNF in human neuroblastomas. Mol Cell Biol 1994, 14:759–767
22. Nakagawara A, Nakamura Y, Ikeda H, Hiwasa T, Kuida K, Su MS, Zhao H, Cnaan A, Sakiyama S: High levels of expression and nuclear localization of interleukin-1 beta converting enzyme (ICE) and CPP32 in favorable human neuroblastomas. Cancer Res 1997, 57:4578–4584
23. Posmantur R, McGinnis K, Nadimpalli R, Gilbertsen RB, Wang K: Characterization of CPP32-like protease activity following apoptotic challenge in SH-SY5Y neuroblastoma cells. J Neurochem 1997, 68:2328–2337
24. Adida C, Berrebi D, Peuchmaur M, Reyes-Mugica M, Altieri DC: Anti-apoptosis gene, survivin, and prognosis of neuroblastoma. Lancet 1998, 351:882–883
25. Hiyama E, Hiyama K, Yokoyama T, Matsuura Y, Piatyszek MA, Shay JW: Correlating telomerase activity levels with human neuroblastoma outcomes. Nat Med 1995, 1:249–255
26. Lamant L, Pulford K, Bischof D, Morris SW, Mason DY, Delsol G, Mariame B: Expression of the ALK tyrosine kinase gene in neuroblastoma. Am J Pathol 2000, 156:1711–1721
27. Miyake I, Hakomori Y, Shinohara A, Gamou T, Saito M, Iwamatsu A, Sakai R: Activation of anaplastic lymphoma kinase is responsible for hyperphosphorylation of ShcC in neuroblastoma cell lines. Oncogene 2002, 21:5823–5834
28. Sakai R, Henderson JT, O'Bryan JP, Elia AJ, Saxton TM, Pawson T: The mammalian ShcB and ShcC phosphotyrosine docking proteins function in the maturation of sensory and sympathetic neurons. Neuron 2000, 28:819–833
29. Perucho M, Goldfarb M, Shimizu K, Lama C, Fogh J, Wigler M: Human-tumor-derived cell lines contain common and different transforming genes. Cell 1981, 27:467–476
30. Brodeur GM, Pritchard J, Berthold F, Carlsen NL, Castel V, Castelberry RP, De Bernardi B, Evans AE, Favrot M, Hedborg F, Kaneko M, Kemshead J, Lampert F, Lee RE, Look AT, Pearson AD, Philip T, Roald B, Sawada T, Seeger RC, Tsuchida Y, Voute PA: Revisions of the international criteria for neuroblastoma diagnosis, staging, and response to treatment. J Clin Oncol 1993, 11:1466–1477
31. Shimada H, Ambros IM, Dehner LP, Hata J, Joshi VV, Roald B, Stram DO, Gerbing RB, Lukens JN, Matthay KK, Castleberry RP: The International Neuroblastoma Pathology Classification (the Shimada system). Cancer 1999, 86:364–372
32. Ikeda I, Ishizaka Y, Tahira T, Suzuki T, Onda M, Sugimura T, Nagao M: Specific expression of the ret proto-oncogene in human neuroblastoma cell lines. Oncogene 1990, 5:1291–1296
33. Motegi A, Fujimoto J, Kotani M, Sakuraba H, Yamamoto T: ALK receptor tyrosine kinase promotes cell growth and neurite outgrowth. J Cell Sci 2004, 117:3319–3329
34. Slamon DJ, Clark GM, Wong SG, Levin WJ, Ullrich A, McGuire WL: Human breast cancer: correlation of relapse and survival with amplification of the HER-2/neu oncogene. Science 1987, 235:177–182
35. Tsuda H, Hirohashi S, Shimosato Y, Hirota T, Tsugane S, Yamamoto H, Miyajima N, Toyoshima K, Yamamoto T, Yokota J, Yoshida T, Sakamoto H, Terada M, Sugimura T: Correlation between long-term survival in breast cancer patients and amplification of two putative oncogene-coamplification units: hst-1/int-2 and c-erbB-2/ear-1. Cancer Res 1989, 49:3104–3108
36. Ganju P, O'Bryan JP, Der C, Winter J, James IF: Differential regulation of SHC proteins by nerve growth factor in sensory neurons and PC12 cells. Eur J Neurosci 1998, 10:1995–2008
37. Nakamura T, Komiya M, Gotoh N, Koizumi S, Shibuya M, Mori N: Discrimination between phosphotyrosine-mediated signaling properties of conventional and neuronal Shc adapter molecules. Oncogene 2002, 21:22–31
38. Nakamura T, Muraoka S, Sanokawa R, Mori N: N-Shc and Sck, two neuronally expressed Shc adapter homologs: their differential regional expression in the brain and roles in neurotrophin and Src signaling. J Biol Chem 1998, 273:6960–6967
39. O'Bryan JP, Songyang Z, Cantley L, Der CJ, Pawson T: A mammalian adaptor protein with conserved Src homology 2 and phosphotyrosine-binding domains is related to Shc and is specifically expressed in the brain. Proc Natl Acad Sci USA 1996, 93:2729–2734
40. Pelicci G, Troglio F, Bodini A, Melillo RM, Pettirossi V, Coda L, De Giuseppe A, Santoro M, Pelicci PG: The neuron-specific Rai (ShcC) adaptor protein inhibits apoptosis by coupling Ret to the phosphatidylinositol 3-kinase/Akt signaling pathway. Mol Cell Biol 2002, 22:7351–7363
41. Yuan J, Yankner BA: Apoptosis in the nervous system. Nature 2000, 407:802–809
42. De Vita G, Melillo RM, Carlomagno F, Visconti R, Castellone MD, Bellacosa A, Billaud M, Fusco A, Tsichlis PN, Santoro M: Tyrosine 1062 of RET-MEN2A mediates activation of Akt (protein kinase B) and mitogen-activated protein kinase pathways leading to PC12 cell survival. Cancer Res 2000, 60:3727–3731

Available online at www.sciencedirect.com
SCIENCE DIRECT®
Cancer Letters 228 (2005) 29–35
CANCER Letters
www.elsevier.com/locate/canlet

Functional implication of p73 protein stability in neuronal cell survival and death

Toshinori Ozaki[a], Mitsuchika Hosoda[a,b], Kou Miyazaki[a], Syunji Hayashi[a,b], Ken-ichi Watanabe[a,b], Takahito Nakagawa[a,b], Akira Nakagawara[a,*]

[a]*Division of Biochemistry, Chiba Cancer Center Research Institute, 666-2 Nitona, Chuoh-ku, Chiba 260-8717, Japan*
[b]*Department of General Surgery, Hokkaido University School of Medicine, Sapporo 060-8638, Japan*

Received 26 November 2004; accepted 2 December 2004

Abstract

p73, a newly identified member of *p53* family, locates at human chromosome 1p36.2-3, a region which is frequently deleted in a wide variety of human tumors including neuroblastoma. p73 is induced to be accumulated in response to a subset of DNA damaging agents such as cisplatin, and thereby promoting G1/S cell cycle arrest and/or apoptosis. Since the expression levels of p73 are kept extremely low under normal conditions, stabilization of p73 is critical for its effects on cell growth inhibition and apoptosis. Indeed, p73 is induced at protein level in SH-SY5Y neuroblastoma cells exposed to cisplatin. Several lines of evidence indicate that stress-induced post-translational modifications of p73 such as phosphorylation and acetylation lead to a marked extension of its half-life. p73 stability is regulated at least in part by proteasome-dependent degradation pathway, however, MDM2 which mediates ubiquitination and subsequent degradation of p53 by the 26S proteasome, does not promote the proteolytic degradation of p73, implying that the protein stability of p73 is regulated through a pathway distinct from that of p53. Although little is known about the regulation of p73 turnover, we are now beginning to understand the regulatory mechanisms by which p73 is induced to be stabilized in response to apoptotic stimuli, and exerts its pro-apoptotic activity. In this review, we discuss about the cellular proteins implicated in the stability control of p73.

Keywords: E3 ubiquitin ligase; MDM2; Neuroblastoma; p53; p73; p63; Proteasome; Ubiquitination; UFD2a

1. Introduction

p73 belongs to the tumor suppressor p53 family including p53, p73 and p63 [1,2]. As expected from their structural similarity, particularly in the central sequence-specific DNA-binding domain (over 60% amino acid sequence identity), p73 displays several p53-like properties. Analogous to p53, p73 can transactivate a large number of p53-responsive genes such as $p21^{WAF1}$ and *Bax*, and thereby inducing G1/S cell cycle arrest and/or apoptosis in a variety of cancerous cells [3]. *p73* gene has been mapped to human chromosome 1p36.2-3, a region which is frequently lost in neuroblastoma and other types of

* Corresponding author. Tel.: +81 43 264 5431; fax: +81 43 265 4459.
E-mail address: akiranak@chiba-cc.jp (A. Nakagawara).

0304-3835/$ - see front matter © 2005 Elsevier Ireland Ltd. All rights reserved.
doi:10.1016/j.canlet.2004.12.050

tumors [1]. In a sharp contrast to p53, however, p73 is rarely mutated in human tumors including neuroblastoma despite an extensive search [4], and the loss of p73 does not predispose mice to cancer [5], suggesting that p73 does not function as a classic Knudson-type tumor suppressor. Recently, it has been demonstrated that the p53-dependent apoptosis requires the indirect contribution of at least one of the other p53 family members, p73 or p63 [6], whereas p73 is sufficient to induce apoptosis in the absence of p53 [7,8]. Thus, it is likely that p73 cooperates with p53 to induce apoptosis and/or exerts its pro-apoptotic activity in a p53-independent manner. These findings have emphasized the functional importance of p73 in the regulation of apoptotic response, and attracted considerable attention. In particular, p73 is regarded as an important cell fate determinant of neuroblastoma in response to apoptotic stimuli, because wild-type p53 lacks its intact function due to its abnormal cytoplasmic localization in neuroblastoma [9].

Unlike p53, p73 is expressed as multiple variants with varying COOH-terminal extensions (TA isoforms) and lacking NH_2-terminal transactivation domain (ΔN isoforms), arising from alternative splicing and promoter usage, respectively (Fig. 1) [3]. Among them, ΔNp73 has an oncogenic potential [10], and exhibits a dominant-negative behavior toward TAp73 as well as p53 [5,11]. Consistent with this notion, the expression levels of ΔNp73 are closely associated with poor prognosis in human tumors including neuroblastoma [12,13]. Intriguingly, we and others found that p73 directly transactivates the expression of ΔNp73, suggesting that there exists a negative feedback regulation of p73 by ΔNp73 to modulate cell survival and death [14,15].

Steady-state expression levels of endogenous p73 are maintained at extremely low level under normal conditions, keeping this dangerous protein in an inactive state. In response to a subset of genotoxic stresses including oncotoxic drug cisplatin and ionizing radiation, however, p73 is induced to be accumulated at protein level, and the stabilization of p73 results in either G1/S cell cycle arrest or commitment to death through apoptosis [16]. Thus, stabilization of p73 is directly linked with its function. Several pieces of evidence suggest that the protein stability of p73 is regulated through a pathway distinct from that of p53 [8,17]. Although p73 protein stability is regulated at least in part by proteasomal degradation [17,18], it remains still unknown whether the proteasome-mediated degradation system is the main degradation route of p73. In this review, we will discuss about the cellular proteins regulating the p73 stability and how they affect its stability and activity.

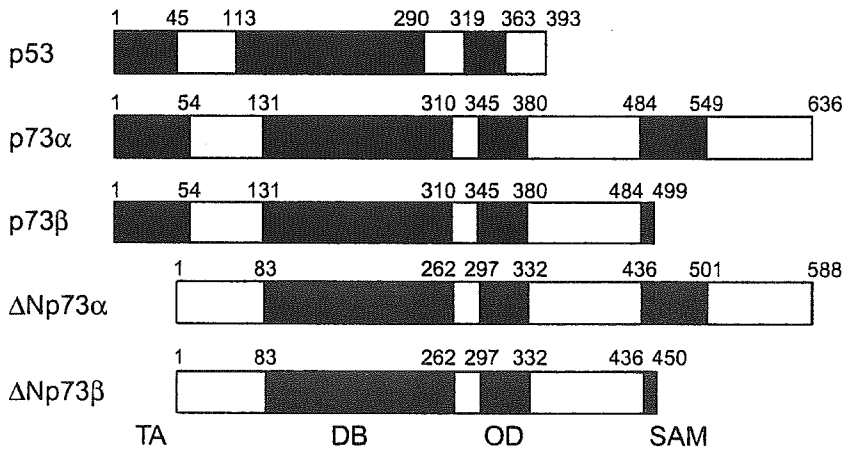

Fig. 1. Structural comparison between p53 and p73. p73α and p73β are generated by alternative splicing. Alternative promoter usage gives rise to ΔNp73α and ΔNp73β. The domains indicated are: a transactivation domain (TA), a DNA-binding domain (DB), an oligomerization domain (OD) and a sterile alpha motif domain (SAM).

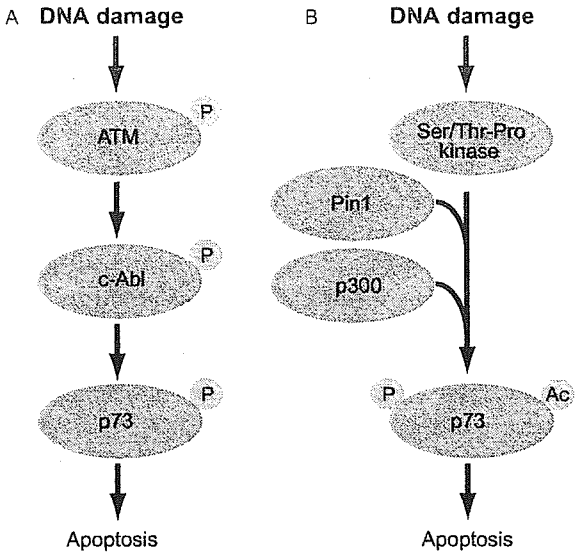

Fig. 2. Chemical modification enhances the stability as well as pro-apoptotic activity of p73 in response to DNA damage. (A) In response to DNA damage, nuclear nonreceptor tyrosine kinase c-Abl is activated by ATM, and thereby phosphorylating p73 at Tyr-99. (B) Pin1 recognizes phosphorylated serine or threonine residues of p73 which can be catalyzed by as yet unidentified Ser/Thr-Pro-directed kinase(s), and enhances its acetylation by p300.

2. Chemical modifications which make p73 stable

Genotoxic stresses including cisplatin treatment and ionizing radiation prolong the half-life of p73 and enhance its pro-apoptotic activity in a pathway dependent on nuclear nonreceptor tyrosine kinase c-Abl [19–21]. According to those results, c-Abl interacts with p73 through the SH3 domain of c-Abl and the p73 PXXP motif, and directly phosphorylates p73 at Tyr-99. Consistent with this notion, p73 is not induced to be accumulated in c-Abl-deficient cells in response to cisplatin (Fig. 2A) [19]. Intriguingly, Ben-Yehoyada et al. found that ionizing radiation induces the tyrosine phosphorylation as well as stabilization of p73 in a c-Abl-dependent manner, and the phosphorylated forms of p73 become associated with the nuclear matrix, suggesting that c-Abl-mediated nuclear redistribution of p73 might play a critical role in the regulation of p73 function [22]. They also described that the amounts of p73 associated with nuclear matrix are increased in the presence of proteasome inhibitor such as MG-132. Alternatively, cisplatin treatment promotes the interaction between p73 and protein kinase Cδ catalytic fragment (PKCδCF) [23]. PKCδCF phosphorylates p73 at Ser-289, and increases its stability. Since PKCδCF enhances the catalytic activity of c-Abl, it is likely that c-Abl could act as a second signal in the functional interaction with p73. Recently, Gonzalez et al. reported that cisplatin-induced apoptosis is associated with the phosphorylation of p73 at Ser-47 catalyzed by Chk1 [24]. Chk1-mediated phosphorylation might convert a latent form of p73 to an active one. Additionally, p73 is phosphorylated at Thr-86 by CDK complexes in a cell cycle-dependent manner [25]. In a sharp contrast to Chk1, the CDK-mediated phosphorylation causes a significant inhibition of the transcriptional activity of p73. Under their experimental conditions, CDK complexes have negligible effect on the amounts of p73.

In addition to the DNA-damage-induced phosphorylation of p73, p73 is regulated by acetylation. Previously, it has been demonstrated that p300 interacts with the NH_2-terminal region of p73, and enhances its pro-apoptotic activity [26]. It is worth noting that doxorubicin treatment induces the acetylation of p73 at Lys-321, Lys-327 and Lys-331 and this acetylation is mediated by p300 in a c-Abl-dependent manner [27]. Based on these results, acetylated form of p73 has a pro-apoptotic activity, whereas nonacetylatable p73 fails to promote apoptosis. Moreover, Mantovani et al. found that p300-mediated acetylation of p73 is enhanced by prolyl isomerase Pin1, and promotes the stabilization of p73 [28]. Pin1 binds to the phosphorylated serine or threonine residue followed by proline of p73, and induces its conformational shift to stimulate the interaction between p73 and p300 (Fig. 2B). Thus, the identification of Ser/Thr kinase(s) required for the phosphorylation of Pin1-binding site on p73 is important to clarify a molecular mechanism underlying the DNA damage-induced stabilization of p73.

3. Ubiquitin-mediated proteolysis of p73

p73 level is dependent on a balance between protein synthesis and degradation. As described by Lee and La Thangue [18], the steady-state expression levels of p73 are significantly increased in the presence of proteasome inhibitor such as LLnL,

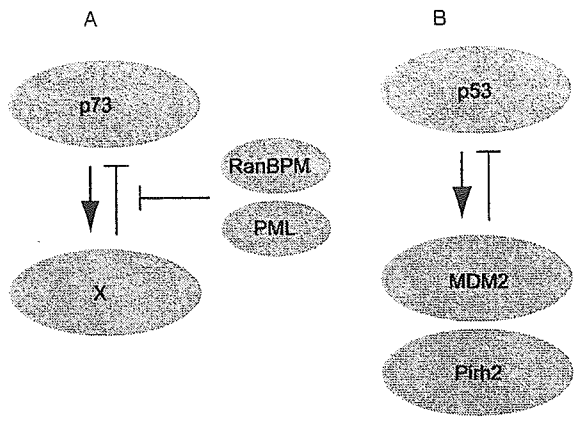

Fig. 3. Ubiquitination-dependent degradation pathway of p73 is distinct from that used for p53. (A) Ubiquitination of p73 could be mediated by p73-induced gene product(s), and significantly inhibited by RanBPM and/or PML. (B) p53-induced E3 ubiquitin ligases MDM2 and Pirh2 promote the ubiquitination and subsequent degradation of p53 by 26S proteasome, however, they have negligible effect on the ubiquitination level of p73.

suggesting that p73 turnover is regulated at least in part by a ubiquitin-dependent proteasome pathway. They also showed that the COOH-terminal extension of p73α is involved in the regulation of protein stability through a pathway that is sensitive to proteasome inhibitor. Recently, we found that RanBPM binds to the extreme COOH-terminal region of p73α, and inhibits its ubiquitination [29]. Of note, Bernassola et al. reported that PML promotes the p300-mediated acetylation of p73, and reduces its ubiquitination levels by competition between acetylation and ubiquitination [30]. In addition, Wu et al. described that the transcriptional activity of p73 is required for its rapid degradation, indicating that the direct transcriptional target(s) of p73 could have an ability to induce its proteolytic degradation (Fig. 3A) [31]. In accordance with this notion, ΔNp73 which lacks the NH_2-terminal transactivation domain, is much more stable than wild-type p73. MDM2 which acts as an E3 ubiquitin ligase for p53, promotes the ubiquitination and subsequent degradation of p53 [32–34]. MDM2 is transcriptionally activated by p53, forming an autoregulatory feedback loop with p53 to tightly regulate its expression levels (Fig. 3B). Similar to p53, p73 stimulates the transcription of MDM2. MDM2 interacts with the NH_2-terminal transactivation domain of p73 and abrogates its transcriptional activity as well as pro-apoptotic function, whereas it fails to mediate the proteolytic degradation of p73 [35,36]. Like p73, p63 is degraded by a proteasome-dependent pathway, however, MDM2 increases the steady-state level of intracellular p63 [37]. Another p53-induced E3 ubiquitin ligase Pirh2 which promotes p53 degradation (Fig. 3B), has no detectable effect on p73 stability [31,38], suggesting that p73 degradation might be mediated by an as yet unidentified E3 ubiquitin ligase(s) distinct from that used for p53 degradation. Intriguingly, Toh et al. described that c-Jun fails to interact with p73 but prolongs the half-life of p73 by preventing its proteasome-dependent degradation [39]. According to those results, the transactivation function of c-Jun is required for the c-Jun-mediated stabilization of p73. Thus, it is likely that c-Jun activates its transcriptional target(s) implicated in the regulation of p73 stability.

4. Ubiquitination-independent degradation of p73

In addition to the ubiquitin-mediated proteasome pathway, p73 degradation is regulated in a ubiquitination-independent manner. Cyclin G which belongs to the cyclin family, has been shown to be one of the transcriptional target genes of p53 [40]. Recently, Ohtsuka et al. demonstrated that cyclin G interacts with p73 and promotes its down-regulation at protein level [41]. siRNA-mediated knock-down of the endogenous cyclin G results in a significant accumulation of p73 in response to DNA damage. Unexpectedly, cyclin G does not increase the amounts of the ubiquitinated forms of p73, suggesting that cyclin G-mediated destabilization of p73 might be regulated through a pathway distinct from the ubiquitination-dependent degradation system. However, the precise regulatory mechanism of p73 stability by cyclin G remains to be elusive.

5. Viral oncoproteins

As described by Marin et al. [42], HEK293 human embryonic kidney and COS monkey kidney cells express the higher levels of p73 as compared with the other cell lines. HEK293 and COS cells are transformed with viral oncoproteins such as adenovirus E1B and

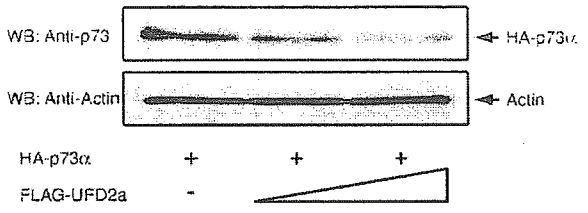

Fig. 4. Down-regulation of p73 by UFD2a. U2OS cells were transiently co-transfected with the indicated combinations of the expression plasmids. Forty-eight hours after transfection, whole cell lysates were prepared and subjected to Western blot analysis (WB) with the indicated antibodies.

simian virus 40 (SV40) T antigen, respectively. In addition, Lemasson and Nyborg reported that HTLV-1-transformed cells express a high level of p73, whereas p73 is undetectable in uninfected T-cell lines [43]. Viral oncoprotein Tax which is encoded by HTLV-I, has an ability to enhance the stability of p73. Since these viral oncoproteins do not interact directly with p73, as yet unidentified indirect mechanism(s) appears to contribute to maintain the higher levels of p73 in those transformed cells. Considering that adenovirus E1A binds to p300 and inhibits its E3/E4 ubiquitin ligase activity to stabilize p53 [44], it is plausible that viral oncoproteins such as E1B, T antigen and Tax could inhibit the enzymatic activity of unidentified E3/E4 ubiquitin ligase for p73 through the physical interaction, and thereby protecting p73 from ubiquitination-mediated proteolytic degradation.

6. Interaction between p73 and UFD2a in human neuroblastoma cell lines

We have previously identified a homozygously deleted region at 1p36.2-p36.3 in neuroblastoma cell line NB-C201 [45]. Within this region, there exist six genes including *DFF45*, *PGD*, *CORT*, *UFD2a*, *KIF1B*-β and *PEX14*. Among them, UFD2a which belongs to the U-box-type ubiquitin ligase family, has an E3 as well as E4 ubiquitin ligase activity [46,47]. It has been shown that UFD2a is implicated in cell survival under a certain stress condition [46]. In response to apoptotic stimuli, UFD2a is cleaved by caspase 6 or granzyme B, and its enzymatic activity is markedly impaired [48]. It is, thus, tempting to speculate that UFD2a might participate in the regulation of cell survival and death.

Recently, we have found that, during the cisplatin-mediated apoptosis in SH-SY5Y neuroblastoma cells, UFD2a is down-regulated at protein level in association with a significant accumulation of p73. Ectopic expression of UFD2a results in a reduction of p73 (Fig. 4), and this observation is supported by a decrease in a half-life of p73 in UFD2a-expressing cells. This is consistent with our additional findings showing that UFD2a inhibits the p73-mediated transcriptional activation and apoptosis [Hosoda et al., manuscript in preparation]. Although it is not known whether UFD2a-mediated degradation of p73 could be regulated in a ubiquitination-dependent manner, it is conceivable that down-regulation of UFD2a in response to cisplatin might augment the p73-dependent apoptosis, and thereby providing a novel strategy for anticancer treatment.

7. Conclusion

In contrast to other types of human tumors, *p53* is rarely mutated in neuroblastoma, however, the aberrant cytoplasmic retention of wild-type p53 renders it nonfunctional. Since p73 has an ability to induce tumor cell apoptosis irrespective of *p53* status, it is likely that p73 is a pivotal player in apoptotic response, particularly in tumors such as neuroblastoma lacking functional p53. Accumulating evidence strongly suggests that p73 is regulated through a pathway distinct from that of p53. In this respect, it is necessary to clarify signaling pathways which specifically regulate the activity as well as stability of p73 in response to apoptotic stimuli.

References

[1] M. Kaghad, H. Bonnet, A. Yang, L. Creancier, J.C. Biscan, A. Valent, et al., Monoallelically expressed gene related to p53 at 1p36, a region frequently deleted in neuroblastoma and other human cancers, Cell 90 (1997) 809–819.
[2] A. Yang, M. Kaghad, Y. Wang, E. Gillett, M.D. Fleming, V. Dotsch, et al., p63, a p53 homolog at 3q27-29, encodes multiple products with transactivating, death-inducing, and dominant-negative activities, Mol. Cell 2 (1998) 305–316.
[3] G. Melino, V. De Laurenzi, K.H. Vousden, p73: friend or foe in tumorigenesis, Nat. Rev. Cancer 2 (2002) 605–615.